Title

EVALUATION OF HIGH-SPEED TWO-TUBE CONFIGURATIONS. PART I: GREATER GAIN-BANDWIDTH IN TRIGGER CIRCUITS. PART II: TRANSIENT ANALYSIS OF THE WHITE CATHODE FOLLOWER

Author

Brown, Melvin.

Publication Date

1959-11-01

UCRL 8954

UNIVERSITY OF CALIFORNIA

Ernest O. Lawrence

Radiation Laboratory

BERKELEY, CALIFORNIA

DISCLAIMER

UCRL-8954

UNIVERSITY OF CALIFORNIA
Lawrence Radiation Laboratory
Berkeley, California

Contract No. W-7405-eng-48

EVALUATION OF HIGH-SPEED TWO-TUBE CONFIGURATIONS:

PART I. GREATER GAIN-BANDWIDTH IN TRIGGER CIRCUITS

PART II. TRANSIENT ANALYSIS OF THE WHITE CATHODE FOLLOWER

Melvin Brown
(Thesis-Master's)

November 1959

Printed for the U.S. Atomic Energy Commission

EVALUATION OF HIGH-SPEED TWO-TUBE CONFIGURATIONS; PART I. GREATER GAIN-BANDWIDTH IN TRIGGER CIRCUITS PART II. TRANSIENT ANALYSIS OF THE WHITE CATHODE FOLLOWER

Contents

EVALUATION OF HIGH-SPEED TWO-TUBE CONFIGURATIONS; PART I. GREATER GAIN-BANDWIDTH IN TRIGGER CIRCUITS PART II. TRANSIENT ANALYSIS OF THE WHITE CATHODE FOLLOWER

Melvin Brown

Lawrence Radiation Laboratory
University of California
Berkeley, California

November 1959

PREFACE

This study is concerned with a class of circuits which employs two tubes in a series connection--sometimes referred to as the stacked-tubes connection. Depending upon the particular interconnection of the two tubes, one tube may replace either the plate load resistance or the cathode resistance of the other tube. External circuitry often provides ac feedback from one tube to the other.

A great number of different configurations are possible but this study will be concerned with two that have shown considerable promise in the field of high speed circuitry. In Part I a configuration called the dynamic plate load amplifier is dealt with. In Part II a configuration called the White cathode follower is examined.

EVALUATION OF HIGH-SPEED TWO-TUBE CONFIGURATIONS: PART I. GREATER GAIN-BANDWIDTH IN TRIGGER CIRCUITS PART II. TRANSIENT ANALYSIS OF THE WHITE CATHODE FOLLOWER

Melvin Brown

Lawrence Radiation Laboratory
University of California
Berkeley, California

November 1959

ABSTRACT

In Part I the relation between switching speed of a trigger circuit and the gain band width (GBW) of an amplifier is discussed. A special series connection of two tubes--referred to as a dynamic plate-load amplifier (DPL)--is then presented and analyzed. A dc analysis shows that the DPL investigated has 18% of the output impedance, and 2.75 times the dc gain of a conventional amplifier. A transient analysis shows that the DPL may have 3 times the advantage in GBW over a conventional amplifier. This GBW improvement recommends its utilization in fast trigger circuits. The appendix to Part I provides the regeneration analysis of the DPL trigger circuit.

In Part II is described the White cathode follower, a two-tube series device that provides output impedances of the order of 5 ohms and transmits pulses of either polarity with minimal distortion. A dc and transient analysis of the White cathode follower is made and a typical circuit analyzed. The effect on the transient response of varying the circuit parameters is discussed. Throughout the paper the White cathode follower is compared to the well-known conventional cathode follower. The White cathode follower may have an advantage in gain bandwidth over the conventional cathode follower by a factor of five.

PART I

GREATER GAIN-BANDWIDTH IN TRIGGER CIRCUITS

Melvin Brown

Lawrence Radiation Laboratory
University of California
Berkeley, California

November 1959

1. INTRODUCTION

The speed of transition of a trigger circuit from one state to another is dependent upon (1) the rate at which an active device charges or discharges the circuit capacitances and (2) the rate at which the passive circuit elements such as the capacitors charge and discharge through their associated resistors.

Generally, in a circuit where the active device, such as a vacuum tube, is permitted to go into cut-off, the time constants of the passive elements determine the switching speed. However, it may be shown that to obtain the maximum speed of operation, it is necessary that the active device be operating at all times.[1]

This paper is concerned with vacuum tubes as the active device and presupposes that they will be conducting at all times so as to retain a minimal transconductance. The method usually employed to insure this manner of operation is to clamp the plate and (or) grid swings with biased diodes.

Now it is well known that the speed of switching of an active device is directly dependent on its gain-bandwidth product, abbreviated GBW, as an amplifier.[2] Attempts to increase the GBW of a circuit by directly paralleling tubes have been unsuccessful because as the transconductance increases, the shunt capacitance increases in the same proportion. However, the special parallel connection of tubes in a distributed amplifier does increase the GBW. Unfortunately, the time delay between the input and output of distributed amplifiers prevents their utilization in regenerative switching circuits.

Herein is described a vacuum-tube configuration in which tubes are connected so as to produce a GBW per stage of up to three times that of a conventional amplifier without introducing the unwanted time delay associated with the distributed amplifier.

2. DYNAMIC PLATE-LOAD CIRCUIT

The circuit to be described has been presented by Valley and Wallman as an output circuit for direct-coupled amplifiers without reference to its transient response.[3] It has been used recently in a binary which has resolution in excess of 40 Mc.[4]

The basic configuration is shown in Fig. 1 and will be referred to as a dynamic plate-load circuit (DPL).

The analysis will be in two parts: dc (low frequency) analysis where the tube and circuit capacitances are neglected (Section 3), and transient analysis where the capacitances are included (Section 4). The gain and output-impedance equations of the dc analysis agree with those presented by Valley and Wallman. However, since the method of analysis differs from that in Valley and Wallman, and the results of the dc analysis are used to provide the transient characteristics of the circuit, it is included here for completeness.

3. DC ANALYSIS

The equivalent circuit without the shunt capacitances of the DPL is shown in Fig. 2. The tubes, which for simplicity of analysis are identical, are replaced by equivalent voltage generators.

Of interest in the dc analysis is the gain and output impedance of the circuit. The method of approach will be to set up loop equations based upon the equivalent circuit of Fig. 2 and to solve for the desired quantities by determinants.

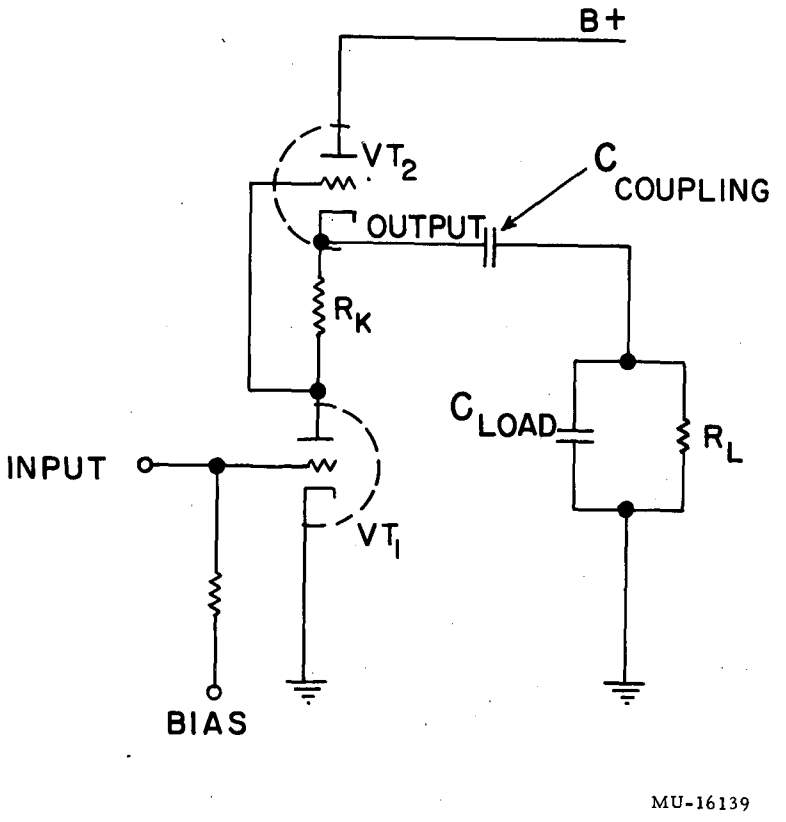

Fig. 1. Schematic of the dynamic plate-load circuit (DPL).

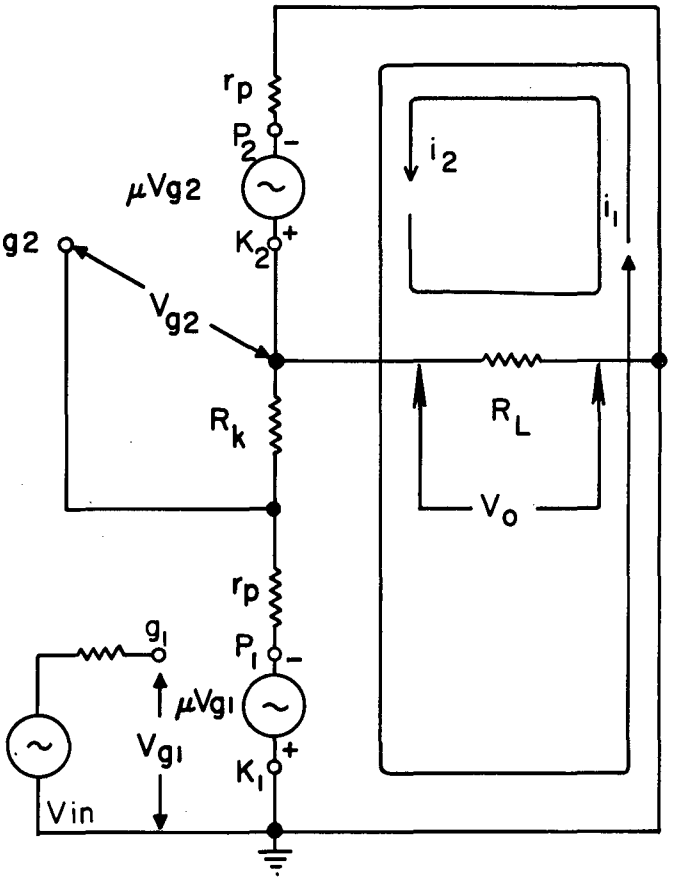

MU-16141

Fig. 2. Equivalent circuit of DPL.

In Loop 1 we have

$$i_1 [2r_p + R_k] + i_2 r_p = \mu[v_{g1} + v_{g2}] \tag{1}$$

where

$$v_{g2} = - i_1 R_k . \tag{2}$$

Substituting Eq. (2) into Eq. (1) and rearranging terms, we obtain

$$i_1 [2r_p + (\mu + 1) R_k] + i_2 r_p = \mu v_{g1} . \tag{3}$$

In Loop 2 we have

$$i_1 r_p + i_2 [r_p + R_L] = \mu v_{g2}$$

$$= \mu (-i_1 R_k) . \tag{4}$$

Rearranging Eq. (4) we obtain

$$i_1 [r_p + \mu R_k] + i_2 [r_p + R_L] = 0 . \tag{5}$$

Solving for i_2 by Cramer's rule from Eqs. (3) and (5), we find

$$i_2 = \frac{\begin{vmatrix} 2r_p + (\mu + 1) R_k & \mu v_{g1} \\ r_p + \mu R_k & 0 \end{vmatrix}}{\begin{vmatrix} 2r_p + (\mu + 1) R_k & r_p \\ r_p + \mu R_k & r_p + R_L \end{vmatrix}} \tag{6}$$

Expanding Eq. (6) and simplifying, we obtain

$$i_2 = - \frac{\mu v_{g1} (r_p + \mu R_k)}{r_p^2 + R_k r_p + (\mu + 1) R_k R_L + 2 r_p R_L} \tag{7}$$

Now the dc gain is

$$\frac{v_o}{v_{g1}} = \frac{i_2 R_L}{v_{g1}} ; \tag{8}$$

Hence, substituting Eq. (7) in Eq. (8) and rearranging, we obtain

$$\frac{v_o}{v_{g1}} = - \frac{\mu (r_p + \mu R_k)}{\frac{r_p}{R_L}(r_p + R_k) + (\mu + 1) R_k + 2r_p} \quad , \tag{9}$$

Now for comparison, the gain expression of a conventional amplifier is

$$\frac{v_o}{v_g} = \frac{\mu R_L}{R_L + r_p} \quad . \tag{10}$$

Since the conventional amplifier will be referred to often, for the sake of clarity its well known physical and equivalent circuit are shown in Fig. 3.

It is now desirable to plot Eqs. (9) and (10) with R_L and R_k as varying parameters for a dual triode 6BQ7 (Fig. 4).

Both identical halves of a 6BQ7 are used in the DPL, while one half of the same tube is used in the conventional amplifier. It is seen in Fig. 4 that, as R_k gets larger and R_L is held constant, the gain advantage of the DPL increases. However as R_k gets larger it increases the grid bias on the upper tube and tends to cutoff the tube, or at least it will decrease the anode current. This decreased anode current reduces the g_m and μ of the tube. In order to offset the reduced anode current, the B+ voltage may be increased until the maximum anode-voltage rating is reached. Thus in the case of the 6BQ7 an anode current of 7.5 ma and an R_k of 560 ohms were the maximum values which satisfied the above conditions.

The tube parameters that were substituted into Eqs. (9) and (10) were directly measured at an anode current of 7.5 ma. These parameters are: r_p = 6100 ohms, g_m = 7000 μmhos, and μ = 43.

The curves of Fig. 4 have been verified by direct measurement. The results show that for low-load resistances the DPL has considerably more gain than the conventional amplifier. In particular for the case we will be interested in later, with an R_L of 1000 ohms and an R_k of 560 ohms the DPL has 2.75 times the dc gain of the conventional amplifier.

We now desire to obtain the output impedance of the DPL. It may be shown that to obtain the output impedance of a two-port device it is

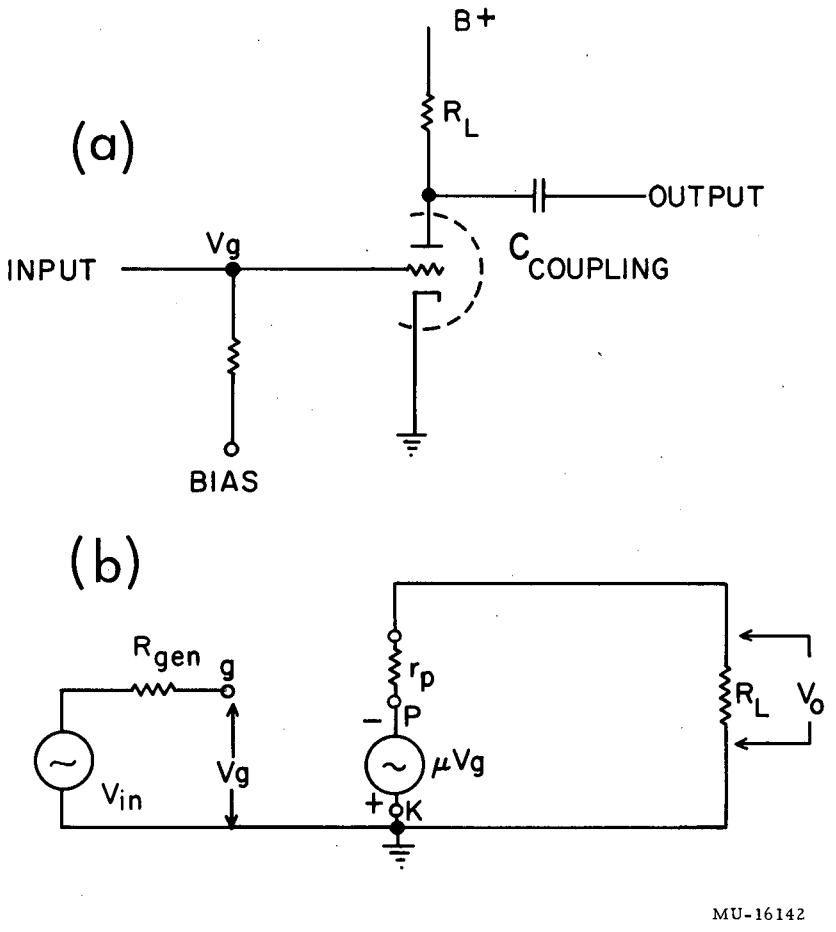

Fig. 3. Conventional amplifier: (a) Physical circuit, (b) Equivalent circuit.

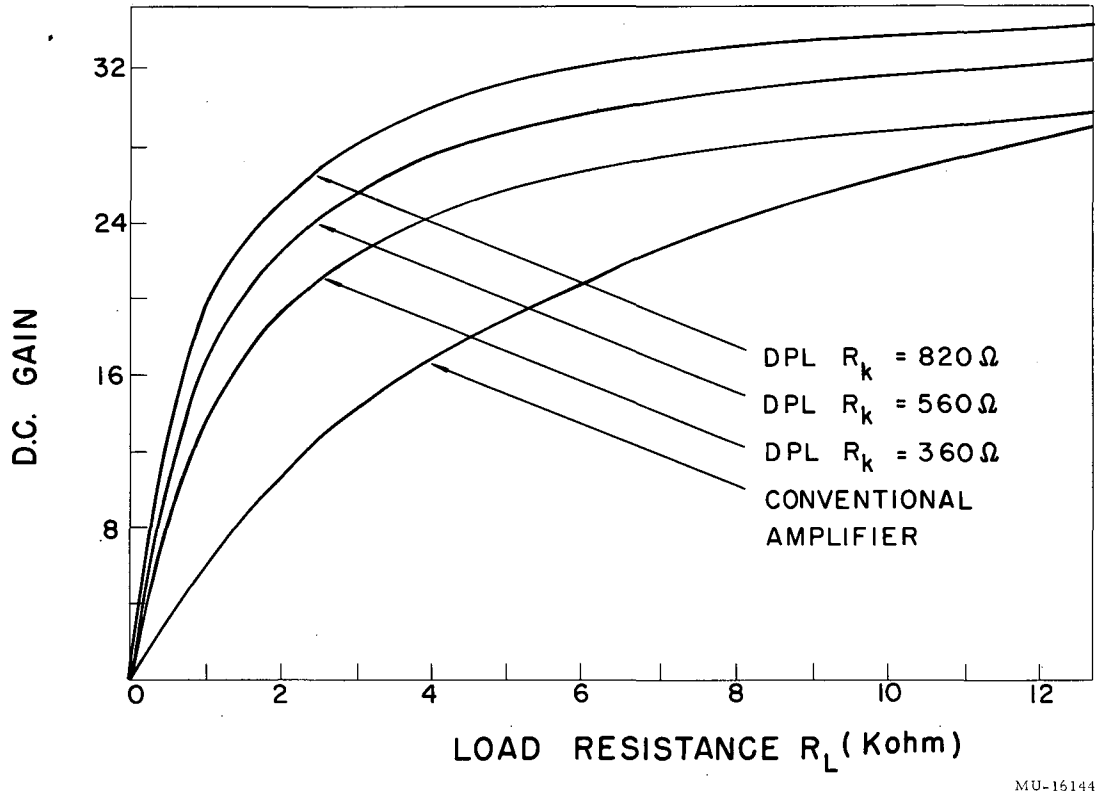

Fig. 4. Comparison of the dc gain of the DPL with that of a conventional amplifier for a 6BQ7 tube.

necessary only to short-circuit the input and to drive the output with a voltage source.[5] The output impedance is then the ratio of the driving voltage to the current leaving this source. The equivalent circuit to obtain the output impedance is shown in Fig. 5.

The equation for Loop 1 of Fig. 5 is

$$i_1 (2r_p + R_k) + i_2 (r_p) = \mu v_{g2} \qquad (\mu v_{g1} = 0)$$
$$= \mu (-i_1 R_k). \tag{11}$$

Rearranging Eq. (11), we obtain

$$i_1 (2r_p + (\mu + 1) R_k) + i_2 r_p = 0. \tag{12}$$

For Loop 2, we have

$$i_1 r_p + i_2 r_p = \mu v_{g2} - v_2$$
$$= \mu (-i_1 R_k) - v_2 , \tag{13}$$

which can be rearranged to

$$i_1 (r_p + \mu R_k) + i_2 r_p = - v_2 . \tag{14}$$

Solving Eqs (12) and (14) for i_2 by Cramer's rule, we obtain

$$i_2 = \frac{\begin{vmatrix} 2r_p + (\mu + 1) R_k & 0 \\ r_p + \mu R_k & -v_2 \end{vmatrix}}{\begin{vmatrix} 2r_p + (\mu + 1) R_k & r_p \\ r_p + \mu R_k & r_p \end{vmatrix}} \tag{15}$$

Expanding Eq. (15) and simplifying, we have

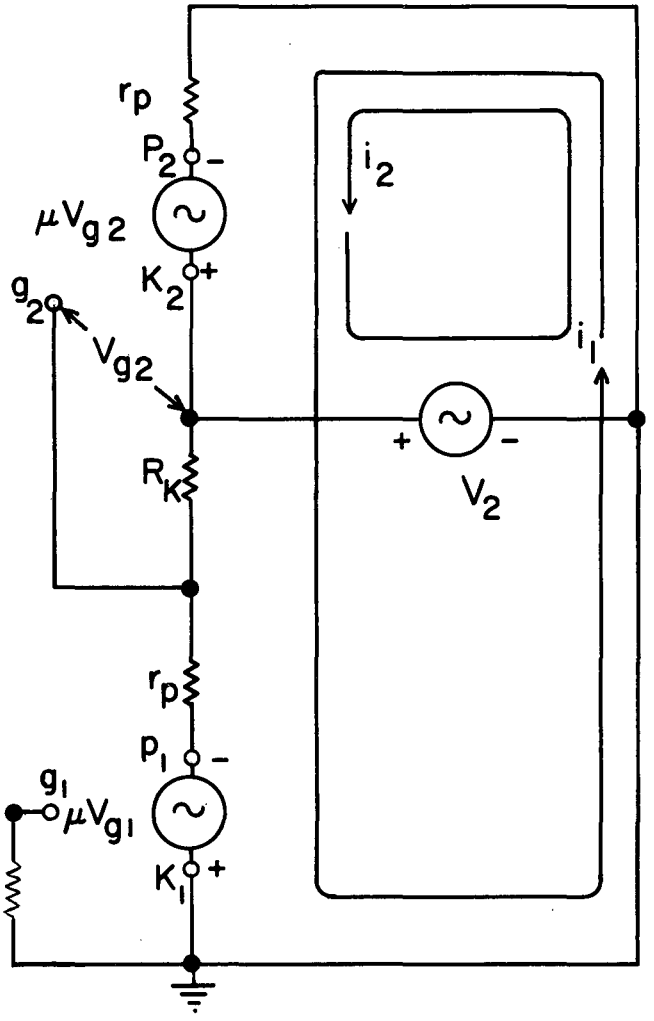

MU-16140

Fig. 5. Equivalent circuit of DPL to obtain the output impedance.

$$i_2 = -\frac{v_2 [2r_p + (\mu + 1) R_k]}{r_p [r_p + R_k]} \qquad (16)$$

Now the output impedance is

$$Z_{22} \equiv \frac{v_2}{i_2} \qquad (17)$$

Hence, from Eq. (16) and (17) we obtain

$$Z_{22} = \frac{r_p (r_p + R_k)}{2r_p + (\mu + 1) R_k} \qquad (18)$$

A plot of Eq. (18) with R_k as the independent parameter is shown in Fig. 6. This curve has been verified by direct measurements. With an R_k = 560 ohms, the output impedance, Z_{22}, is 1100 ohms. This is approximately 18% of the output impedance of the conventional amplifier, which is 6100 ohms.

4. TRANSIENT ANALYSIS OF THE DPL

For simplicity of analysis, the current-generator equivalent circuit will be used for the transient analysis.

The physical circuit is shown in Fig. 7a where the various shunt capacitances are included. The equivalent circuit of Fig. 7a is shown in Fig. 7b. Note the identities between the equivalent capacitances in the legend of Fig. 7b and the physical capacitances of Fig. 7a. Also it should be observed that G_3 is a parallel combination of the current-generator shunt conductance and the load conductance.

In the analysis which follows, C_{in} of Fig. 7b includes the Miller capacitance of the lower tube. This capacitance as well as the generator internal impedance R_g is neglected in the following analysis, because we are assuming that $R_g C_{in}$ is a much smaller time constant than any other in the system.

The method of analysis will be to write the nodal equations and then to obtain the system transfer function. The location of the poles of the system then will be determined by setting the denominator of the transfer

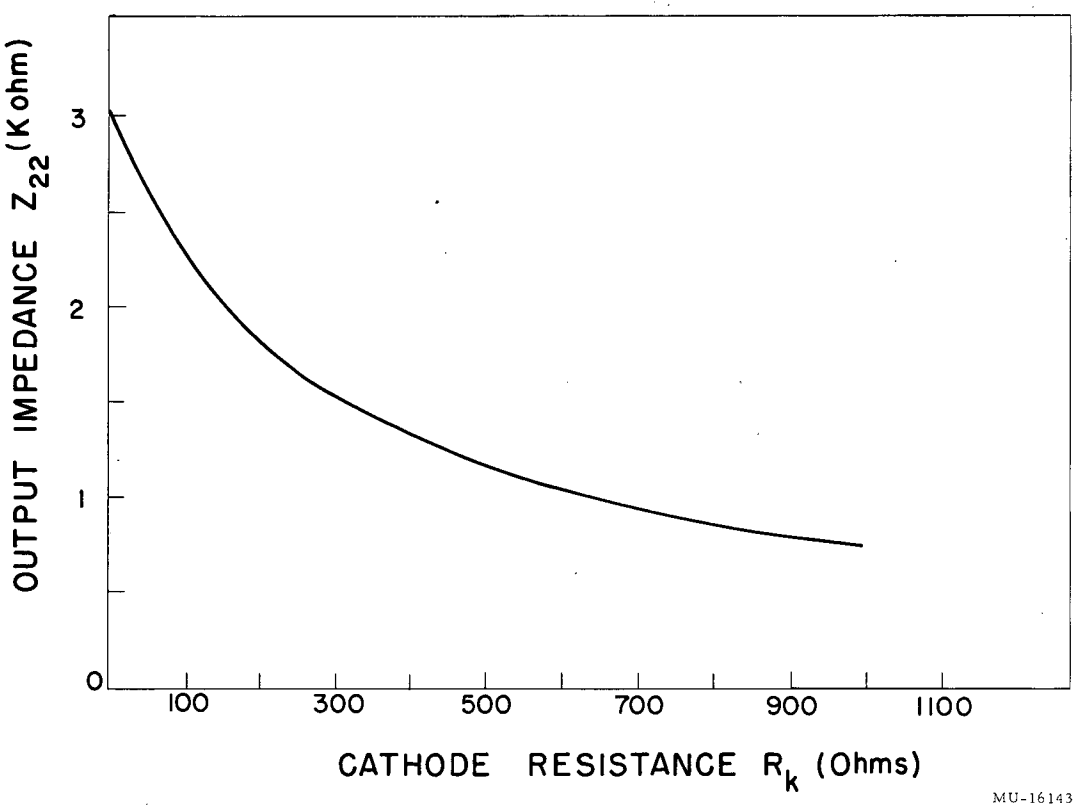

Fig. 6. Output impedance vs. cathode resistance for a 6BQ7 DPL.

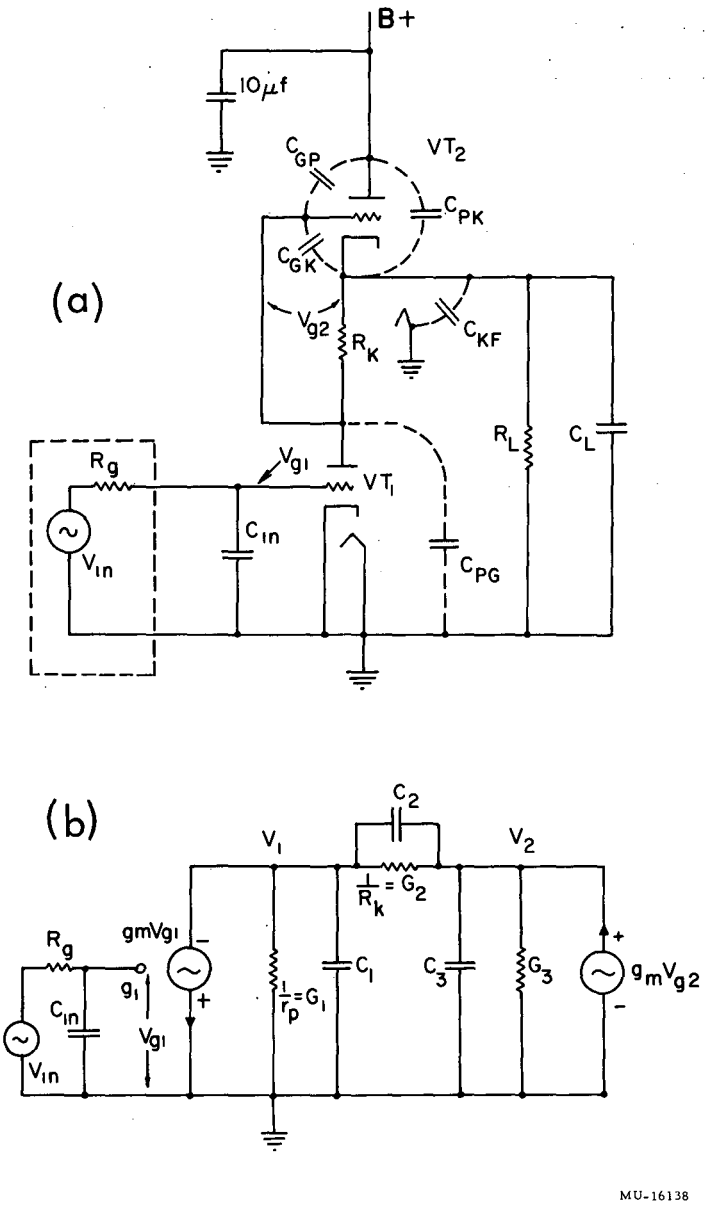

Fig. 7. (a) Schematic of DPL showing capacitances.
(b) Equivalent circuit of DPL with $C_1 = C_{PG} + C_{GP} + C_{Stray}$, $C_2 = C_{GK} + C_{Stray}$, $C_3 = C_{KF} + C_{PK} + C_{Stray} + C_L$, and $G_3 = (R_L + r_P) / (R_L \cdot r_P)$.

function equal to zero. It will be shown that one of the poles is dominant. The product of this pole, and the dc gain will give the gain-bandwidth of the system.

The nodal equations are

$$v_1 [p(C_1 + C_2) + G_1 + G_2] - v_2[pC_2 + G_2] = - g_m v_{g1} \tag{19}$$

and

$$-v_1 [pC_2 + G_2] + v_2 [p(C_2 + C_3) + G_2 + G_3] = g_m v_{g2}. \tag{20}$$

Now noting that

$$g_m v_{g2} = - g_m [v_2 - v_1] \tag{21}$$

and substituting Eq. (21) into Eq. (20), we obtain

$$-v_1[pC_2 + G_2 + g_m] + v_2[p(C_2 + C_3) + G_2 + G_3 + g_m] = 0. \tag{22}$$

Solving for v2 by Cramer's rule with Eqs. (19) and (22), we obtain

$$v_2 = \frac{\begin{vmatrix} p(C_1 + C_2) + G_1 + G_2 & -g_m v_{g1} \\ -[pC_2 + G_2 + g_m] & 0 \end{vmatrix}}{\begin{vmatrix} p(C_1 + C_2) + G_1 + G_2 & -[pC_2 + G_2] \\ -[pC_2 + G_2 + g_m] & p[C_2 + C_3] + G_2 + G_3 + g_m \end{vmatrix}} \tag{23}$$

Expanding Eq. (23) and rearranging, we obtain

$$v_2/v_{g1} = [-g_m(pC_2 + G_2 + g_m)] \; / \; \{p^2[C_3(C_2 + C_1) + C_1C_2]$$

$$+ p[C_1(G_2 + G_3) + C_2(G_1 + G_3) + C_3(G_1 + G_2) + C_1g_m]$$

$$+ G_1(G_2 + G_3 + g_m) + G_2G_3 \} \quad . \tag{24}$$

Now the location of the poles of the transfer function v_2/v_{g1} may be obtained by setting the denominator of Eq. (24) equal to zero. Hence we have

$$p^2 + p \left[\frac{C_1(G_2 + G_3) + C_2(G_1 + G_3) + G_3(G_1 + G_2) + C_1 g_m}{C_3(C_2 + C_1) + C_1 C_2} \right]$$

$$\frac{G_1(G_2 + G_3 + g_m) + G_2 G_3}{C_3(C_2 + C_1) + C_1 C_2} = 0 . \qquad (25)$$

It is now desirable to illustrate a typical calculation involving Eq. (25). The values of the capacitances of Fig. 7a were measured with a Tektronix Model 130 LC meter and are, in μμf:

$$C_{GP} = 1.7$$

$$C_{PK} = 1.9$$

$$C_{GK} = 3.3$$

$$C_{KF} = 3.6$$

$$C_{PG} = 1.9 .$$

These values include the socket capacitances. Care was exercised in using the guard voltage of the LC meter so as to isolate the above capacitances from each other.

In addition there are stray capacitances due to the physical components and the output connections. These values were also measured and are added to the above capacitances to obtain the values for the equivalent circuit. Hence, from the identities of Fig. 7b, the equivalent circuit capacitances are, in μμf:

$$C_1 = C_{PG} + C_{GP} + C_{Stray} = 1.9 + 1.7 + 2.0 = 5.60$$

$$C_2 = C_{GK} + C_{Stray} = 3.3 + 1 = 4.3$$

$$C_3 = C_{KF} + C_{PK} + C_{Stray} + C_L = 3.6 + 1.9 + 5.2 + C_L$$

$$= 10.7 + C_L .$$

Now choosing $R_k = 560$ ohms and $R_L = 1000$ ohms, the conductances of Fig. 7b are, in μmhos:

$$G_1 = \frac{1}{r_p} = \frac{1}{6100} = 164$$

$$G_2 = \frac{1}{R_k} = \frac{1}{560} = 1790$$

$$G_3 = \frac{R_L + r_p}{R_L r_p} = \frac{10^3 + 6.1\times 10^3}{6.1\times 10^6} = 1170.$$

Normalizing the above conductances by dividing by 10^{-3} and the capacitances by multiplying by 10^{12} and substituting them in Eq. (25), we obtain

$$p^2 + \frac{p(1.95\, C_L + 82.5)}{9.95\, C_L + 130} + \frac{3.73}{9.90\, C_L + 140.3} = 0. \qquad (26)$$

For the one remaining substitution a normalized load capacitance, C_L, of 25 farads is chosen and Eq. (26) is solved for its roots. Thus we obtain $p_1 = 0.032$ and $p_2 = 0.312$.

Since p_1 is one-tenth as far as p_2 from the origin of the p plane then p_1 may be considered a dominant pole. Substituting other values of C_L into Eq. (26) will show that p_1 is always at least ten times closer to the p-plane origin than p_2. Therefore p_2 will be neglected, and p_1 will be considered the only pole that affects the bandwidth of the system. It may be shown that in a one-pole system, the numerical value of the pole is identical with the 3-db bandwidth in units of radians per second.[6]

Now denormalizing p_1 and dividing by 2π to convert to cycles per second, we obtain

$$BW = \frac{p_1 \times 10^9}{2\pi} = 4.94 \text{ Mc.}$$

The dc gain may be determined from Fig. 4 or Eq. (9) for $R_L = 1000$ ohms. Thus the gain is 16.8. Hence GBW_{DPL} is $16.8 \times 4.94 = 83.0$ Mc.

Now for a conventional amplifier we have

$$BW = \frac{G_{Total}}{2\pi C_{Total}} , \tag{27}$$

where

$$G_{Total} = \frac{R_L + r_p}{R_L r_p}$$

and

$$C_{Total} = C_{Tube} + C_{Strays} + C_{Load} .$$

Substituting into Eq. (27) the same load resistance and capacitance as in the DPL example above and using measured values of C_{Tube} and C_{Strays}, we obtain

$$BW = \frac{1.17 \times 10^{-3}}{2\pi (1.9 + 4.1 + 25) \times 10^{-12}} = 6.01 \text{ Mc.}$$

The dc gain for the conventional amplifier obtained from Fig. 4 or Eq. (10) is 6.05. Hence, we have

$$GBW_{Conv.\ Ampl.} = 6.05 \times 6.01 = 36.4 \text{ Mc.}$$

Similar computations of GBW were made for other values of load capacitance for both the DPL and conventional amplifier and the results are plotted in Fig. 8. The curves of Fig. 8 show the advantage of the DPL over the conventional amplifier. The GBW improvement is a function of load capacitance and varies approximately from 80% with $C_L = 15\mu\mu f$ to 200% with $C_L = 55\mu\mu f$. The lack of substantial improvement of the DPL at very low load capacitances (around 5 $\mu\mu f$) may be accounted for by considering all the additional tube and stray capacitances present in the DPL in contrast to those present in the conventional amplifier. However, at larger load capacitances the tube and stray capacitances are masked out, and the DPL shows its advantage. Furthermore, in physical trigger circuits the load capacitance is generally greater than 5 to 10 $\mu\mu f$, and the above theoretical limitation is often not pertinent.

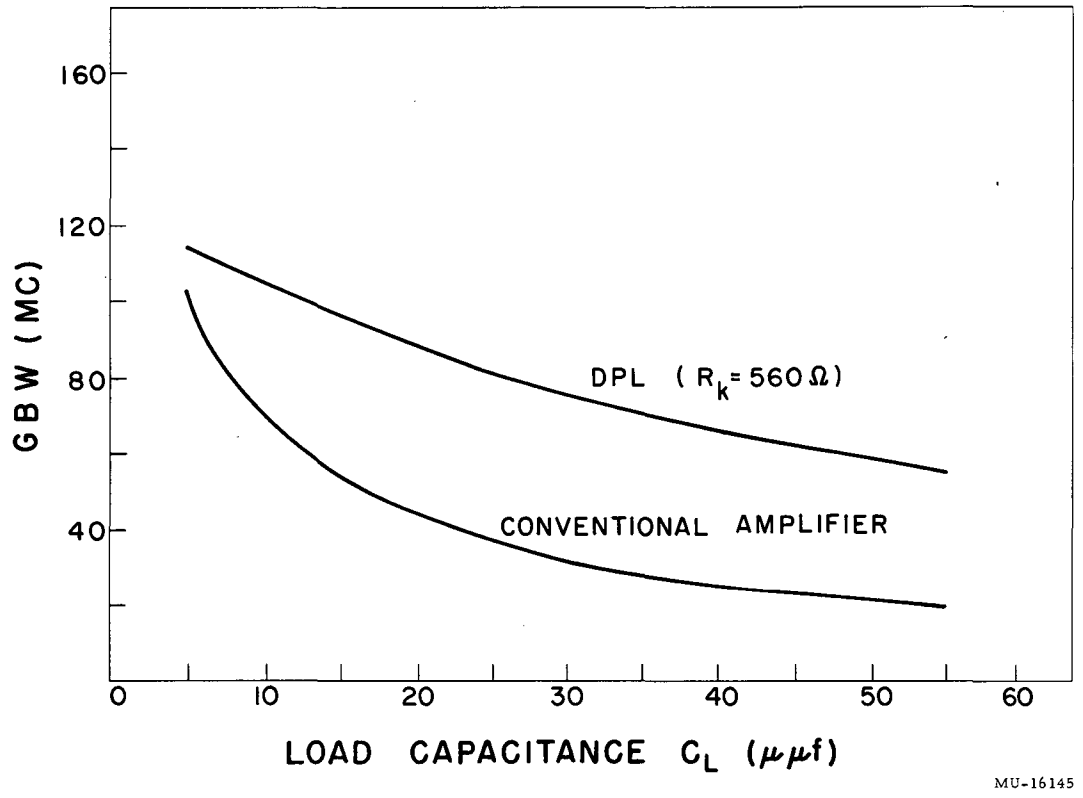

Fig. 8. Theoretical comparison of GBW of the DPL and conventional amplifier for a 6BQ7 tube.

The question of the optimum value of R_k to obtain maximum GBW is of interest. Simple calculations show that an increase of R_k decreases the bandwidth less than it increases the dc gain; therefore R_k should be as large as possible. The upper limit on the value of R_k has been discussed in the dc analysis (Section 3).

5. EXPERIMENTAL RESULTS

Experimental confirmation of Fig. 8 has been obtained by observing the pulse response of the DPL and conventional amplifier whose parameters were given in the previous section. The same tube was used for both tests. In each case the anode current was 7.5 ma and the signal input bias voltage was -0.5 v. The dc gain of the DPL measured 16.5 and the load resistance of the conventional amplifier was adjusted to give the same gain. The pulse response to a 0.2 v negative step input pulse as the load capacitance is varied is shown in Fig. 9.

The pulse source was a mercury-relay pulse generator with an internal impedance of 125 ohms and a rise time of a fraction of a mμs. The photos were taken on a Tektronix 517 A oscilloscope which has a rise time of 7 mμs. These photos were magnified 24 times to permit careful measuring of the 10 to 90% rise time.

Translating rise time to bandwidth by using $BW = 0.35/T_R$ and multiplying the result by the dc gain, we obtain the experimentally measured GBW plotted in Fig. 10. This may be compared to the theoretical results of Fig. 8.

The maximum error between experimental and theoretical GBW occurs at the lowest values of load capacitance and is approximately 16% for the DPL. As the load capacitance is increased the error decreases to about 6% at $C_L = 55\mu\mu f$. Examination of Eq. (25) will show that the tube and stray capacitances contribute heavily to the value of GBW at low load capacitances. Therefore it would appear that there were errors in the measurement of the tube and stray capacitances for the equivalent circuit. It would further seem that large load capacitances mask out these tube and stray capacitances, and thus their contributory error to the GBW is minimized. Substitution of other values of tube and stray capacitances into Eq. (25) will show that

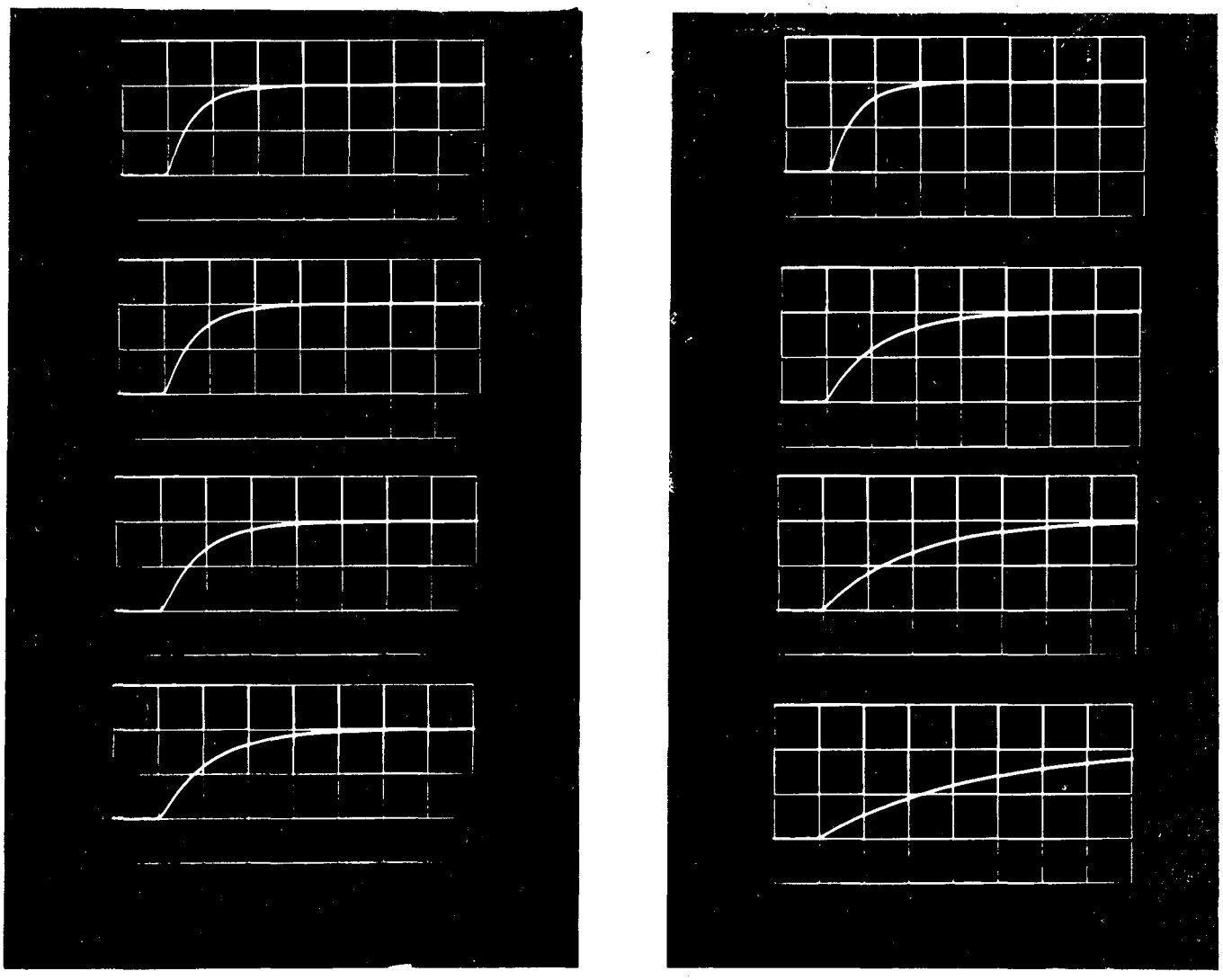

ZN-2047

Fig. 9. Rise time of DPL (left) and conventional amplifier (right) as load capacitance is varied (sweep speed: 50 mμs/cm; pulse amplitude: 3.3 v). Values of C_L are (top to bottom) 5μμf, 15μμf, 30μμf, and 55μμf.

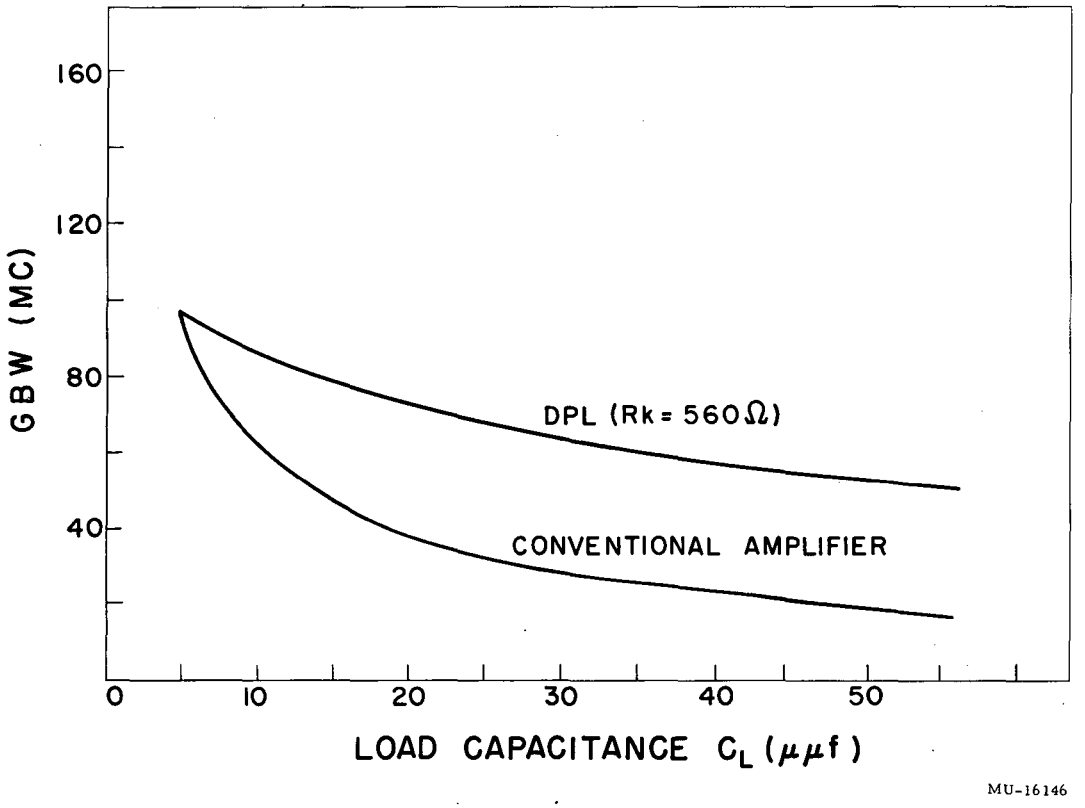

Fig. 10. Experimental GBW of DPL and conventional amplifier for a 6BQ7 tube.

the above interpretation is valid. The GBW product is relatively insensitive to even a 25% change in the tube and stray capacitances when the load capacitance is large.

6. PHYSICAL CONCEPT OF THE DPL

It is desirable to obtain some physical picture of the DPL to explain its advantage. At the risk of oversimplification an attempt will be made to do so.

One way to understand the advantage of the DPL over the conventional amplifier is by considering the results of the dc analysis. The low output impedance of the DPL is in parallel with the external load resistance and capacitance. This low impedance constrains the parallel combination to have a short time constant.

Another (or possible similar) way of looking at the DPL is to consider the ratio of internal voltage-generator impedance of the DPL to its load impedance. In the DPL, the voltage drop across the internal generator impedance is less than in a conventional amplifier. Hence more voltage is available at the output terminals, providing more gain and consequently a greater GBW. The essential advantage appears to rest in the lower output impedance of the DPL.

Because the plate load of the lower tube is an active device (another tube), and it is this active device that accounts for the lower output impedance, the name dynamic (or active) plate load suggested itself.

7. FURTHER CONSIDERATIONS

Shunt peaking may be employed in the DPL as in a conventional amplifier. However, in the DPL the inductance is placed in series with the cathode resistance, R_k, instead of in series with the load resistance. It has been found experimentally that the same relative advantage in GBW may be obtained in the DPL as in a conventional amplifier by shunt peaking.

The tube used for comparison above was medium-mμ dual-triode 6BQ7. If such a tube is used in one side of a regenerative trigger circuit, the formerly neglected Miller capacitance should be considered as part of the load capacitance of the other tube. If pentodes are used, the neglect of the Miller capacitance is, of course, fully justified.

It has been found experimentally and by calculations for the DPL that varying the load resistance, R_L, has little effect on the GBW with a given load capacitance, C_L. That is, if the gain is halved by decreasing R_L, the BW is doubled, provided the load capacitance remains the same. However, as may be seen from Fig. 8, GBW is not constant with varying load capacitance for a given R_L. This means that if C_L is halved, the GBW is not doubled at a fixed R_L.

Hitherto no mention has been made of the time delay in the DPL. Inspection of the physical circuits of the DPL and the conventional amplifier indicates no appreciable increase in time delay. A comparison of the circuitry of the DPL and a distributed amplifier (another method for improving GBW) emphasizes the relative insignificance of time delay in the DPL.

8. CONCLUSION

The dc analysis shows that the DPL with a typical value of $R_k = 560$ ohms has an output impedance about 18% that of a conventional amplifier using the same tube type. Furthermore, the dc gain at low load resistances (around 1000 ohms) varies from two to three times that of the conventional amplifier, depending upon the value of R_k.

The transient analysis shows that for one tube type (6BQ7) the DPL may have a factor of three improvement in the GBW over a conventional amplifier. Empirical confirmation of the transient analysis checks to within 18%, and the areas of error between the results have been discussed.

The broadbanding factor in the DPL appears to be R_k, and it should be made as large as possible, the maximum value being determined by the tube type and operating potentials.

All results tend to recommend the utilization of the DPL as the active device in regenerative trigger circuits.

APPENDIX

In order to further illustrate the advantage of the DPL over a conventional amplifier when both types are used in a trigger circuit, the following regeneration analysis is appended.

Two DPL amplifiers as shown in Fig. 7 may be fed back on each other to form a trigger circuit as shown in Fig. 11 below. The nodal equations are:

$$\begin{aligned} av_1 - bv_2 + 0v_3 + g_m v_4 &= 0 \\ -cv_1 + dv_2 + 0v_3 + 0v_4 &= 0 \\ 0v_1 + g_m v_2 + av_3 - bv_4 &= 0 \\ 0v_1 + 0v_2 - cv_3 + dv_4 &= 0 \end{aligned} \qquad \text{(A-1)}$$

where

$$\begin{aligned} a &= [p\ (C_1 + C_2\ ) + G_1 + G_2] \\ b &= [pC_2 + G_2] \\ c &= [pC_2 + G_2 + g_m] \\ d &= [p(C_2 + C_3) + G_2 + G_3 + g_m] \end{aligned} \qquad \text{(A-2)}$$

The location of the natural frequencies of regeneration may be found by setting the system determinant equal to zero. Hence from Eqs. (A-1) and (A-2) we obtain*

$$p^2 + p\left[\frac{C_1\ (G_2 + G_3) + C_2(G_1 + G_3) + C_3\ (G_1 + G_2) + g_m\ (C_1 \pm C_2)}{C_3(C_2 + C_1) + C_1C_2}\right] + \frac{G_1\ (G_2 + G_3 + g_m) + G_2(G_3 \pm g_m) \pm g_m^{\,2}}{C_3(C_2 + C_1) + C_1C_2} = 0 \qquad \text{(A-3)}$$

---

* The notation (a ± b) here means (a + b) (a - b).

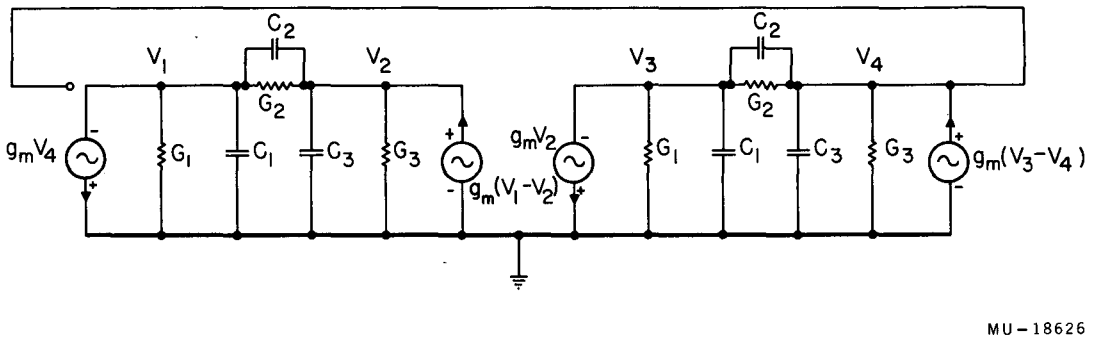

Fig. 11. Equivalent DPL trigger circuit for regeneration analysis.

It is interesting to note that Eq. (A-3) is quite similar to the characteristic equation of the open-loop system given by Eq. (25). The positive root of Eq. (A-3) corresponds to a growing transient which essentially determines the switching speed.

Now a similar analysis will be made of a conventional amplifier trigger circuit. The equivalent schematic is shown if Fig. 12. The nodal equations are:

$$(pC + G)v_1 - g_m v_2 = 0 \qquad (A-4)$$

$$-g_m v_1 + (pC + G)v_2 = 0. \qquad (A-5)$$

When the system determinant is set equal to zero, we obtain

$$p_1 = \frac{g_m - G}{C} \qquad (A-6)$$

and

$$p_2 = -\frac{g_m + G}{C}, \qquad (A-7)$$

where p_1 is the natural frequency of regeneration.
Now the time required for the anode voltage to increase ten times is given by[7]

$$T_r = \frac{2.2}{p} \qquad (A-8)$$

where p is the natural frequency of regeneration.

The question now arises of the proper values to substitute into Eqs. (A-3) and (A-6). For convenience we will use the values of G, C, and g_m given in the example of page 18. Since the Miller capacitance has been neglected in the conventional amplifier we may justifiably neglect C_{GP}, the grid to plate capacitance of the upper tube, in the DPL circuit. All other values are the same. After substitution of the circuit values into Eqs. (A-3) and (A-6), the natural frequency of regeneration of the DPL trigger circuit is found to be 0.317×10^9 radians/sec and the natural frequency of regeneration of the conventional-amplifier trigger circuit is found to be $0,188 \times 10^9$ radians/sec. Substitution of these natural frequencies into Eq. (A-8) and taking the ratio of rise times shows a 70% improvement in rise time by using the DPL. If the load capacitance C_L is increased to 50μμf (from 25μμf), there

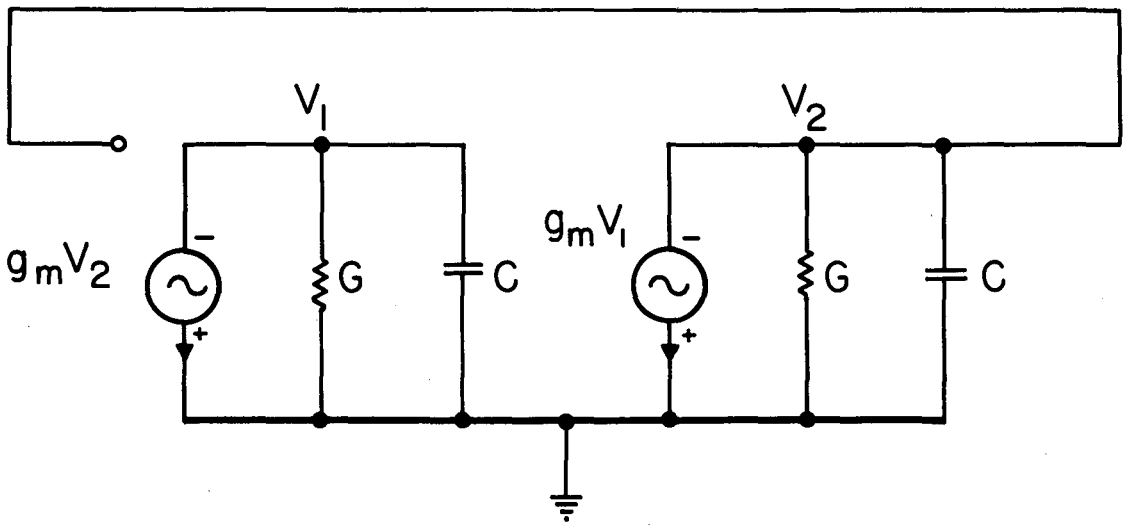

Fig. 12. Equivalent conventional-amplifier trigger circuit for regeneration analysis.

is a 120% improvement in rise time. The improvement in the ratio of the rise times with a larger load capacitance is to be expected from the results of Section 4. . . It should be noted that the above values are very much on the conservative side. A more equitable comparison would be to increase the size of the load resistance of the conventional amplifiers to provide the same magnitude of voltage swing as in the DPL. Then the improvement would be even greater.

The relation between GBW and switching speed may now be discussed. In the above conventional-amplifier regeneration analysis, the GBW (in radians/sec) of the amplifier alone, g_m/C, is explicit in the value of the natural frequency of regeneration (Eq. A-6). When g_m/C is much greater than G/C as is generally the case, then the natural frequency of regeneration is very nearly equal to the GBW of a single amplifier. Hence it is clear that using a conventional amplifier with a higher inherent GBW would increase switching speed.

Now the DPL regeneration analysis does not lend itself so nicely to a simplification that directly relates GBW of the DPL amplifier to switching speed of a DPL trigger circuit. However, if g_m is increased and the capacities decreased, there is an increase of GBW in the DPL amplifier and speed of switching in the DPL trigger circuit. By corollary, when the rise time of a DPL trigger circuit is found to be faster than a comparable conventional-amplifier trigger circuit, it is not unreasonable to attribute this to a greater GBW in the DPL amplifiers. Of course, phase shift is important in a trigger circuit, but this information is contained implicitly in the equations from which GBW was derived.

REFERENCES

1. J. Millman and H. Taub, Pulse and Digital Circuits (McGraw-Hill, New York, 1956), p. 152.
2. Frederick E. Terman, Electronic and Radio Engineering (McGraw-Hill, New York, 1955) p. 288.
3. Vacuum Tube Amplifiers, G. E. Valley, Jr., and H. Wallman, Eds. (McGraw-Hill, New York, 1948) p. 456.
4. Michiyuki Nakamura, Forty-Megacycle Scaler, Rev. Sci. Instr. 28, 1015 (1957).
5. Thomas L. Martin, Jr., Electronic Circuits, (Prentice-Hall, Englewood Cliffs, New Jersey, 1956), p. 92.
6. Martin, loc. cit., p. 117.
7. J. G. Linvill, "Nonsaturating Pulse Circuits Using Two Junction Transistors", Proc. I.R.E., 43, 826 (1955).

PART II

TRANSIENT ANALYSIS OF THE WHITE CATHODE FOLLOWER

Melvin Brown

Lawrence Radiation Laboratory
University of California
Berkeley, California

November 1959

I. INTRODUCTION

The well-known conventional cathode follower (CCF) is shown in Fig. 1. The circuit has been thoroughly analyzed in the literature.[1] It possesses certain inherent limitations of transient response and output impedance that have been overcome by a two-tube series arrangement called a White cathode follower (WCF), which is shown in Fig. 2. The WCF bears the name of Eric L. C. White who patented it in 1944.[2] White claims in his patent that the output impedance of the circuit is low and that it is useful for obtaining a push-pull output without using a transformer. However, no quantitative results are presented.

The dc (or low-frequency) characteristics of the WCF are fairly well-known. In 1946 a low-frequency gain and output impedance analysis of the WCF appeared in the literature.[3] The results of this analysis and some extensions are included below for completeness.

The transient characteristics of the WCF are not so well explored. Occasionally the transient response for a particular WCF is given, but information is lacking as to the effect of various circuit parameters on the transient response. This effect is investigated here and a complete transient analysis of a WCF is given.

An investigation into the input impedance of the WCF as a function of frequency appeared in 1951.[4] It was shown that (as with the CCF) that it is possible to have a negative input resistance at certain frequencies, thus causing oscillation. The elimination of the oscillation is generally effected by the addition of a series grid resistor which cancels the negative resistance.

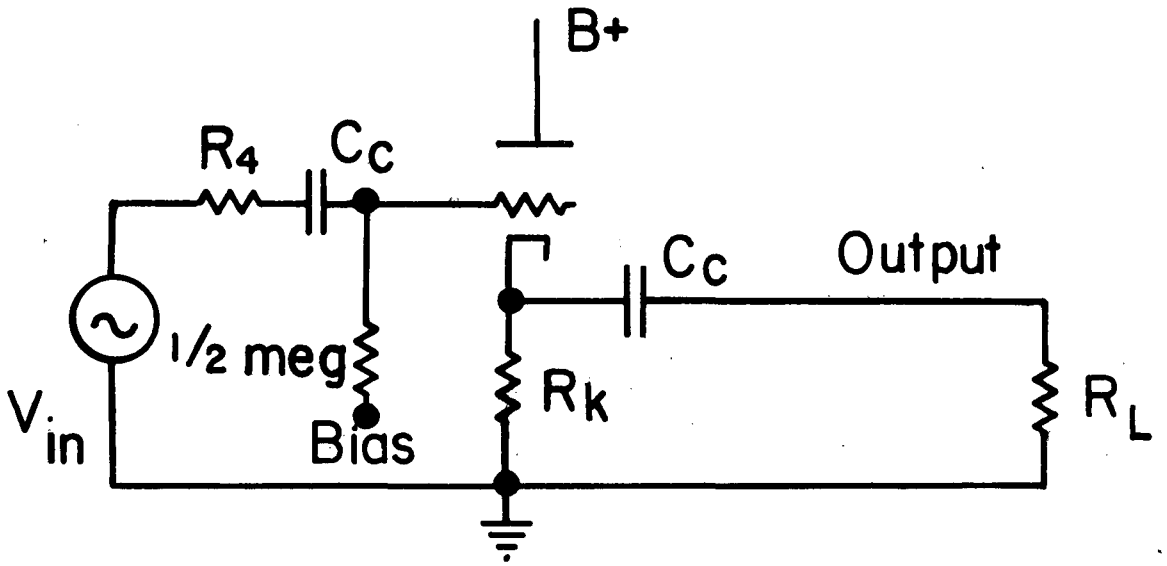

MU-18527

Fig. 1. Conventional cathode follower (CCF). C_c are large coupling capacitors, and R_4 is the source resistance.

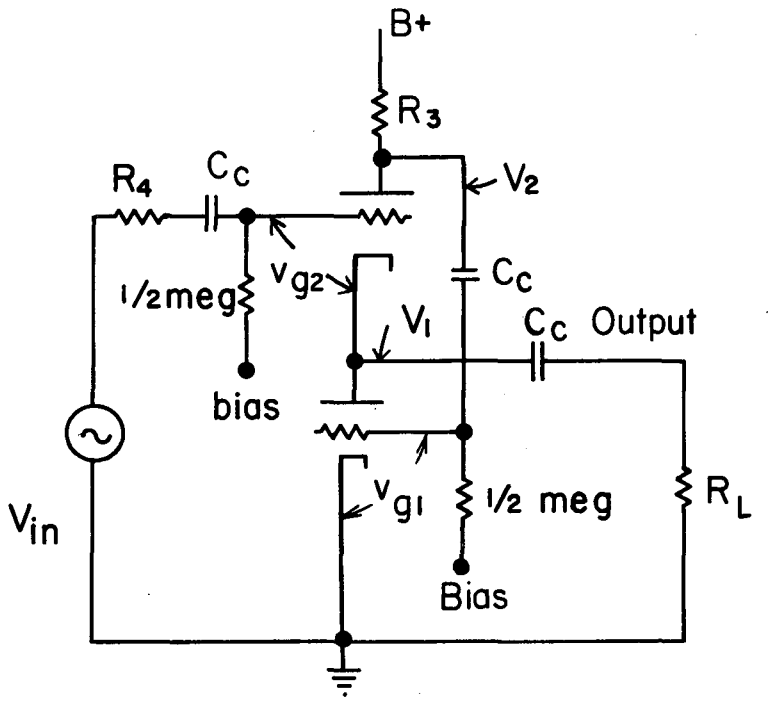

MU-18528

Fig. 2. White cathode follower (WCF). C_c are large coupling capacitors, and R_4 is the source resistance.

In recent years the WCF has become increasingly popular, as shown by its incorporation in various circuits.[5,6,7] Its popularity may be explained by briefly comparing it to a CCF. The response of a CCF to two waveforms that are identical except for an inversion of polarity varies both as to linearity and rise time.[8] The WCF overcomes this problem by virtue of its push-pull circuitry. In addition, the output impedance of the CCF is generally equal to $1/g_m$, about 200 ohms; the output impedance of the WCF may be as low as $1/\mu g_m$, about 5 ohms (g_m is the transconductance and μ is the amplification factor of the vacuum tube).

II. METHOD OF ANALYSIS

The details of the mathematical procedures and techniques of experimental verification, with one exception, are similar to those shown in Part I analyzing another two-tube series configuration.[9] Thus in this paper only light emphasis will be placed upon the mechanics of obtaining the results. The exception to this is the presence of complex poles in the WCF transfer function.

The equations describing the WCF are sometimes long and very cumbersome. Hence, a specific though representative circuit is chosen, and the equations are applied to it. By variation of parameters and graphic presentation of the results, information is made available as to which circuit elements are significant. The specific circuit in this paper employs 6AK5 pentodes which were chosen mainly for convenience. Simplifications arise due to their identical g_m, μ, and r_p (which were measured) as well as the elimination of the grid-to-plate capacity considerations.

Throughout this paper the WCF is compared to the CCF. While it is true that the WCF has two tubes and the CCF has one, the circuits are generally considered for the same application. Where power requirements are of no concern, it is believed that this form of comparison aids in gaining a better understanding of the capabilities of the WCF.

III. DC ANALYSIS

The equivalent circuit for a dc analysis of the WCF is shown in Fig. 3. The relation between the resistances of Fig. 2 and the conductances of Fig. 3 are as follows:

$$G_1 = \frac{1}{r_{p2}} \qquad G_2 = \frac{1}{R_L} + \frac{1}{r_{p1}}$$

$$G_3 = \frac{1}{R_3} \qquad G_4 = \frac{1}{R_4} ,$$

where r_{p1} and r_{p2} are the plate resistances of the lower and upper tubes respectively, R_4 is the driving-source resistance, R_L is the load resistance, and R_3 is the feedback resistance.

Now noting that

$$g_{m1} v_{g1} = g_{m1} V_2 \tag{1}$$

and

$$g_{m2} v_{g2} = g_{m2} (V_{in} - V_1), \tag{2}$$

a nodal analysis yields for the dc gain

$$\frac{V_1}{V_{in}} = \frac{g_{m2} [G_3 + g_{m1}]}{G_1 G_3 + G_2 G_3 + G_2 G_1 + g_{m2} G_3 + g_{m1} G_1 + g_{m1} g_{m2}} . \tag{3}$$

Equation (3) is equivalent to the results of Hammack.[3] Now if the load conductance, $1/R_L$, is much larger than the plate conductance of either tube (such as is the case with pentodes), and if the two tubes are identical, Eq. (3) reduces to approximately

$$\frac{V_1}{V_{in}} = \frac{g_m [G_3 + g_m]}{G_2 G_3 + g_m [G_3 + g_m]} . \tag{4}$$

Next, a loop analysis of the WCF yields for the output impedance

$$Z_{22} = \frac{r_{p1}}{1 + \dfrac{(\mu_2 + 1)(r_{p1} + \mu_1 R_3)}{r_{p2} + R_3}} . \tag{5}$$

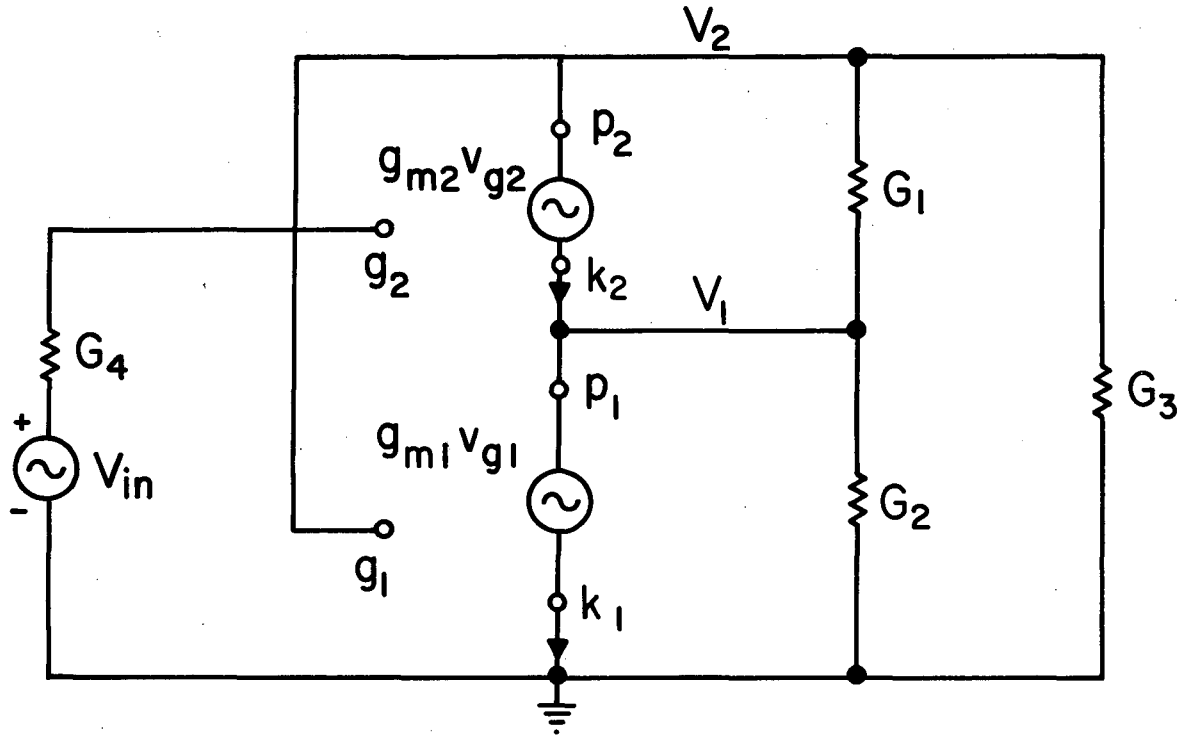

MU-18529

Fig. 3. Equivalent circuit of WCF for dc analysis.

The unilateral nature of the dc characteristics removes the source resistance from the analysis.

If the tubes are identical, R_3 is much larger than r_{p2} and μ is much larger than one, Eq. (5) reduces to

$$Z_{22} = \frac{1}{\mu g_m} . \tag{6}$$

In the case of two identical pentodes, Eq. (5) reduces to approximately

$$Z_{22} = \frac{G_3}{g_m(g_m + G_3)} . \tag{7}$$

A plot of the dc gain vs R_3 $(=1/G_3)$, the feedback resistance, for two 6AK5 tubes (g_m = 5000 μmhos) in a WCF is shown in Fig. 4. It is to be noted that for higher values of R_3 a greater gain is achieved. Also the variation in gain lessens appreciably as R_3 exceeds a few thousand ohms.

A plot of the output impedance vs R_3 for the same WCF is shown in Fig. 5. It is seen that the greater feedback provided by R_3 leads to a lower output impedance. After R_3 exceeds approximately 4000 ohms, the output impedance levels off. The effect of increasing R_3 on the transient response will be dealt with in Section V.

In comparison with the above results for the WCF, the gain for a 6AK5 CCF (g_m = 5000 μmhos) with R_L equal to 125 ohms is 0.385 and with R_L equal to 1000 ohms is 0.835. Furthermore the output impedance of this CCF is about 200 ohms. All the above results have been verified experimentally.

IV. TRANSIENT ANALYSIS

This section is divided into three parts. Part a. deals with the dominant-pole method of analysis. Part b. deals with the transient analysis of the WCF. Because of its length, the general WCF characteristic equation is developed in Appendix A. Part c. deals with the transient analysis of the CCF. The development of the characteristic equation of the CCF is shown in Appendix B.

a. Dominant Poles and Transmission Zeros

The first step in obtaining the transient response of the WCF and

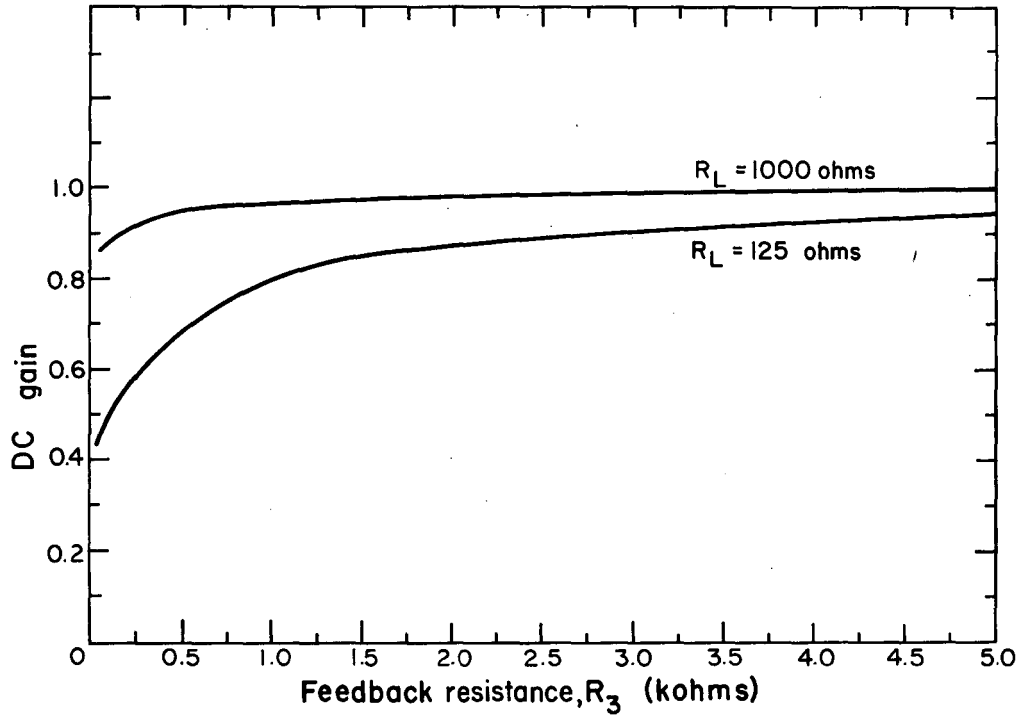

Fig. 4. The dc gain of 6AK5 WCF as the feedback resistance, R_3, is varied.

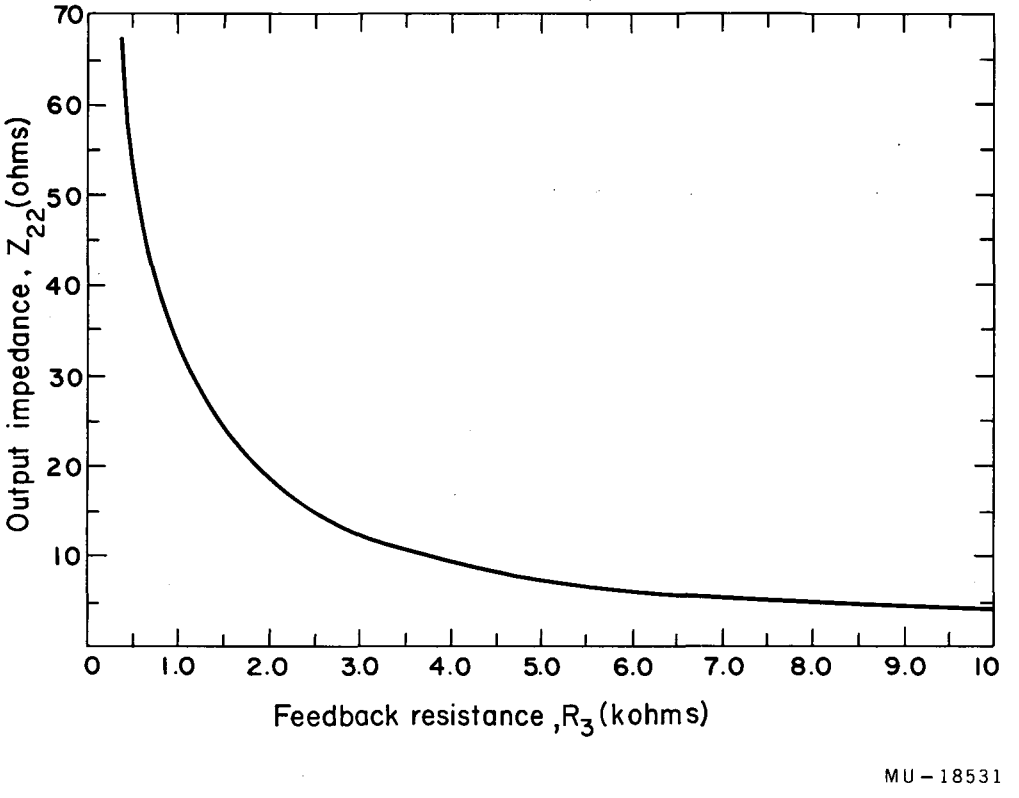

Fig. 5. Output impedance of 6AK5 WCF as the feedback resistance, R_3, is varied.

CCF is to solve for the characteristic equations. Parameters are then substituted into these equations which are solved for their roots (or poles of the transfer function--henceforth referred to simply as poles). If one pole or pair of complex-conjugate poles are dominant, the transient response of the circuit is easily obtained.

In some cases, corresponding to particular circuit parameters, dominant poles cannot be established. The transient response is then obtained from extrapolation between dominant poles which generally bracket the nondominant pole. The question as to what constitutes a dominant pole is of some interest.

A rigorous analysis has been made to establish the dominancy of a pole and to determine the error introduced by disregarding the remaining poles in a system.[10] However, it is usually sufficient to consider one pole or pair of complex-conjugate poles as dominant when it is ten times closer to the origin of the p plane (complex-frequency plane) than any other pole.[11]

The dominant-pole approach is based upon the assumption that the transmission zeros (roots of the numerator of the transfer function) are much further out from the origin of the p plane than the dominant poles. In the case of the WCF, for certain circuit values, transmission zeros are in proximity to dominant poles. If these zeros are ignored and the transient response is obtained by using only dominant poles, the results will show a slower rise time than actually exists. This follows from the fact that poles and zeros that are close tend to cancel each other. In such cases the data is not used, and the transient response is again obtained by extrapolation between dominant poles. If there is some question as to the dominancy of a pole or pair of complex-conjugate poles, a complete inverse Laplace transformation will settle the matter. At times this is a necessary method. The dominant-pole technique is simply an expediency to considerably shorten the work.

In this paper a satisfactory degree of accuracy (within 20%) was obtained by considering a pole or pair of complex-conjugate poles as dominant when it was at least five times closer to the origin of the p plane than any other pole.

b. WCF Analysis

A schematic of the WCF showing the significant capacitances and resistances is shown in Fig. 6. In developing the equivalent circuit of the WCF in Fig. 7 from the schematic of Fig. 6, the following relations are established:

$$C_1 = C_{PG1} + C_{PK2} + C_{stray}$$

$$C_2 = C_{KF2} + C_{PK1} + C_L + C_{stray}$$

$$C_3 = C_{GK1} + C_{stray}$$

C_4 = driving source shunt capacitance

$$C_5 = C_{PG2} + C_{stray}$$

$$C_6 = C_{GK2} + C_{stray},$$

where C_L is the load capacitance.

The relations between the conductances of Fig. 7 and resistances of Fig. 6 are the same as in the dc analysis (Section II).

The nodal equations and the complete transfer function of Fig. 7 are shown in Appendix A. The denominator of Eq. (A-2) set equal to zero is the characteristic equation of the WCF. In the present case of a pentode WCF, certain simplifications are possible. Since C_{PG2} (Fig. 6) is much smaller than any other capacitance in the circuit, C_5 (Fig. 7) may be set equal to zero. Also substitution of terms into Eq. (A-2) will show that G_1, the plate conductance of the upper tube, is negligible in comparison with the other conductances. Hence, the characteristic equation is simplified to

$$p^3 \left[\begin{array}{l} C_4(C_1C_3 + C_2C_3 + C_3C_6 + C_1C_2 + C_1C_6) \\ + C_6(C_1C_3 + C_2C_3 + C_1C_2) \end{array} \right] \qquad (8)$$

$$+ p^2 \left[\begin{array}{l} C_4(C_3G_2 + C_3g_m + C_1G_3 + C_2G_3 + C_6G_3 + C_1g_m + C_1G_2) \\ + C_6(C_3G_2 + C_1G_3 + C_2G_3 + C_1g_m + C_1G_2) \\ + G_4(C_1C_2 + C_3C_2 + C_1C_3 + C_1C_6 + C_3C_6) \end{array} \right]$$

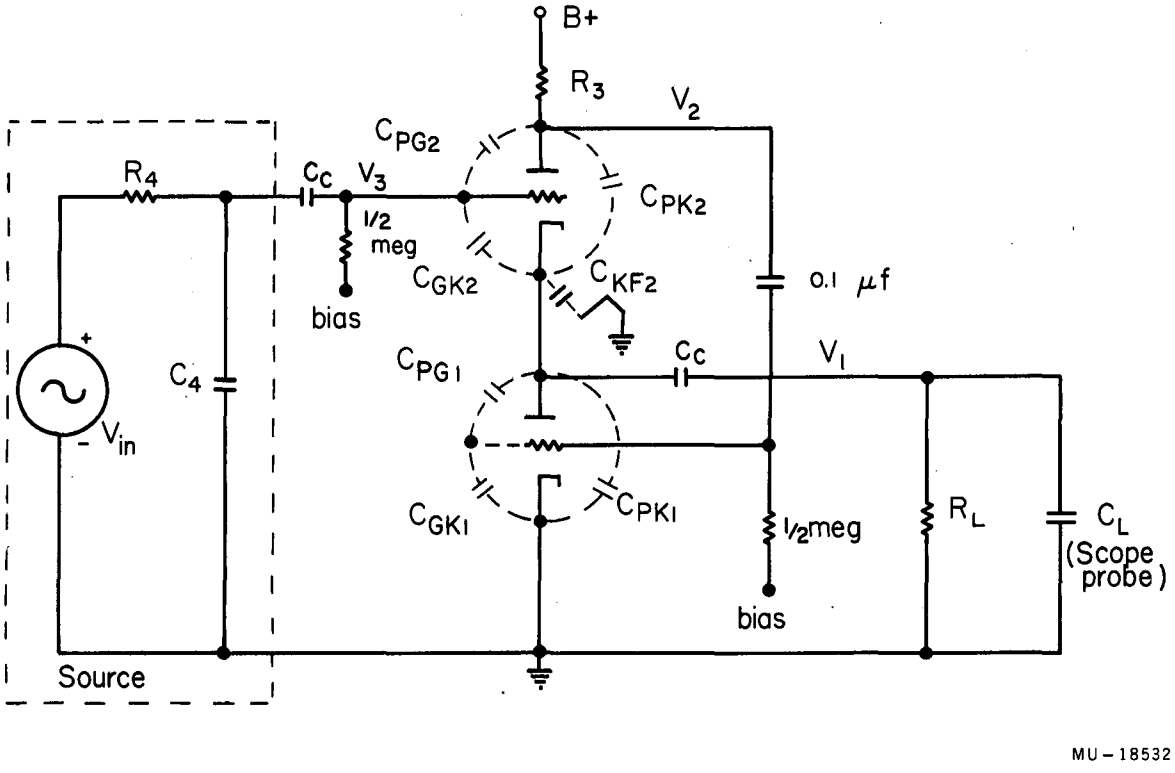

Fig. 6. Simplified circuit of WCF showing essential capacitances for transient analysis.

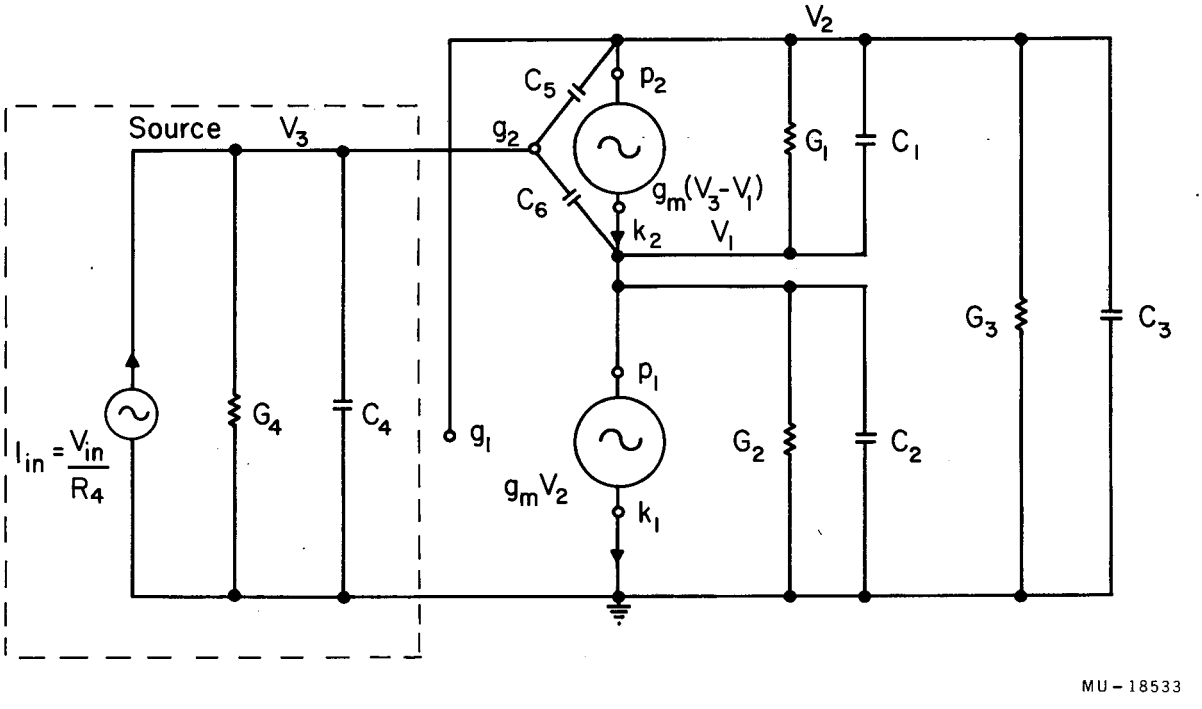

Fig. 7. Equivalent circuit of WCF for transient analysis.

$$+p\left[\begin{array}{l} C_4(G_3G_2 + G_3g_m + g_m^{\,2}) + C_6G_3G_2 + \\ +G_4(C_3G_2 + C_3g_m + C_1G_3 + C_2G_3 + C_1g_m + C_1G_2 + C_6G_3) \end{array}\right]$$

$$+G_4\left[\, G_3G_2 + G_3g_m + g_m^{\,2}\right] = 0 \,. \qquad \text{(8 cont'd)}$$

Furthermore, as G_4, the source conductance, becomes much smaller than any other conductance in the circuit, the last terms in the coefficients of p^2 and p in Eq. (8) become negligible. In this case calculations will show that there is one real dominant pole equal approximately to G_4 divided by the total input capacitance of the cathode follower.

It is now convenient to consider the parameters to be substituted into Eq. (8). If the input and output admittances for the WCF are given, the tubes are usually chosen next. This choice may be dictated by demands of low output impedance, fast transient response or large output currents. A low output impedance follows from a high g_m as shown in the dc analysis (SectionIII). Calculations show that higher g_m tubes lead to a faster transient response. Large currents, which are necessary for large signals across low impedances, are a problem of the emissive capabilities of cathodes and will not be dealt with in this paper. Once the tube is chosen, the g_m and parasitic capacities in the circuit are then known. Apparently, the only remaining parameter which is free to be varied is R_3, the feedback resistance.

However, it is often possible to vary both R_4, the source resistance, and R_L, the load resistance. Indeed, as shown below both these resistances have a vital effect upon the transient response of the WCF, and they are considered to be as significant as R_3. (The source shunt capacitance, C_4 equals 7.5 $\mu\mu$f and the load capacitance C_L equals 5 $\mu\mu$f).

After the above parameters were chosen and measured they were substituted into Eq. (8). Solution of Eq. (8) yields either three real roots (or poles) or one real root and a pair of complex-conjugate roots. These complex roots may lead to overshoot in the transient response to a step input.

When a dominant-pole situation is assumed to exist as described above, the rise time of the WCF is easily calculated by[12]

$$T_r = \frac{2.2}{p_{dom}} . \tag{9}$$

In the case of dominant complex poles, denoted as $\sigma_0 \pm j\,\omega_d$, the characteristic equation may be expressed in quadratic form as

$$(p + \sigma_0 + j\omega_d)\,(p + \sigma_0 - j\,\omega_d) = p^2 + 2\zeta\omega_0 p + \omega_0^2 = 0, \tag{10}$$

where ω_0 is the magnitude of complex frequency, ζ is the damping ratio, $\sigma_0 = \zeta\,\omega_0$ is the real part of the complex frequency, $\omega_d = \omega_0\sqrt{1-\zeta^2}$ is the imaginary part of the complex frequency.

The WCF characteristic equation is now in a standard form familiar in servomechanisms work. The solution of Eq. (10) for rise time, overshoot, settling time, etc. has been dealt with graphically and mathematically in many servomechanisms texts. A graphical solution of Eq. (10), which is taken from a previous reference[13] is used in the present work. In this reference is shown the transient response to a step input with time normalized to ω_0, the independent variable being the damping ratio, ζ. Since the transient response may vary from the overshoot case to the monotonic-rise case as ζ varies, then for convenience the rise time will be taken as the 10 to 90 % value of the final flat top of the step output. The results of the WCF transient analysis are shown below in Section 5.

c. CCF Analysis

The transient analysis of the CCF has been presented in many well-known texts,[14] but the source resistance is generally set equal to zero. In order to compare the WCF with the CCF, it is necessary to perform a transient analysis of the CCF with the source resistance present.

A schematic of a CCF is shown in Fig. 8, and its equivalent circuit is shown in Fig. 9. The nodal equations and the transfer function of the CCF are shown in Appendix B. From Eq. (B-2) the characteristic equation of the CCF is

$$p^2 + p\left[\frac{G_4(C_2 + C_3) + G_2(C_2 + C_4) + g_m C_4}{C_3(C_2 + C_4) + C_2 C_4}\right] + \frac{G_4(G_2 + g_m)}{C_3(C_2 + C_4) + C_2 C_4} = 0. \tag{11}$$

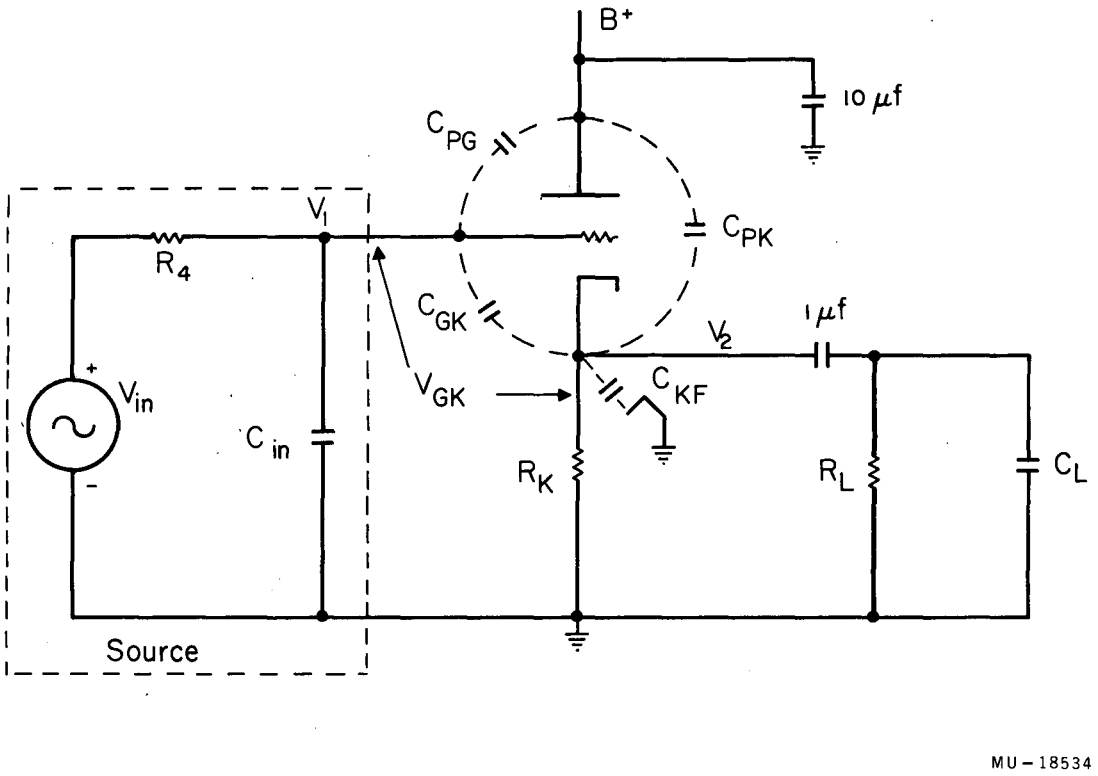

Fig. 8. Schematic of CCF showing essential capacitances for transient analysis.

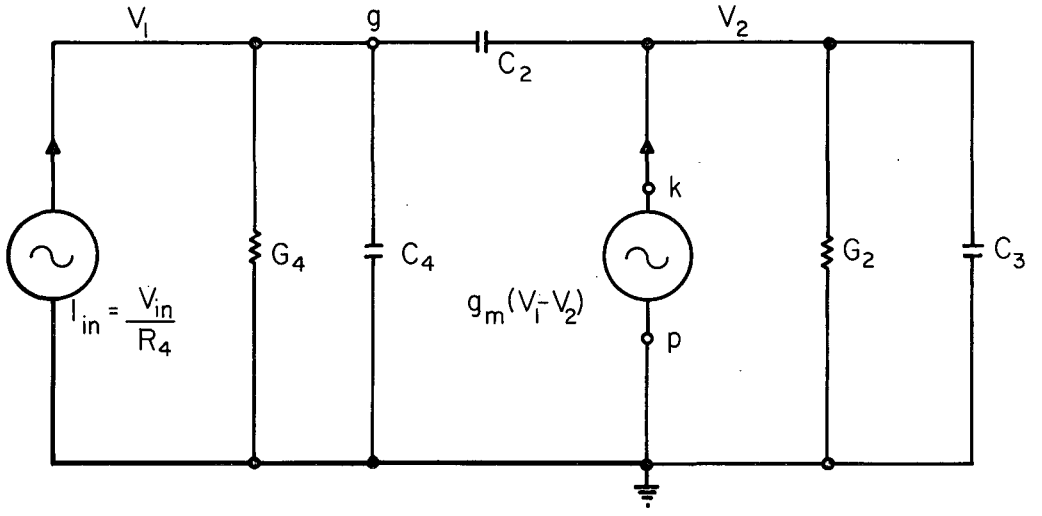

MU-18535

Fig. 9. Equivalent circuit of CCF shown in Fig. 8 with $C_4 = C_{PG} + C_{in} + C_{stray}$; $C_2 = C_{GK} + C_{stray}$; $C_3 = C_{PK} + C_{KF} + C_L + C_{stray}$; and $G_2 = \frac{1}{r_p} + \frac{1}{R_K} + \frac{1}{R_L}$.

It is now desirable to show that a dominant pole generally exists for the CCF. Equation (11) is in the form of $p^2 + ap + b = 0$. Calculations show that if a is much larger than b, a dominant pole exists and is equal to b/a. Since this inequality generally holds for Eq. (11), the dominant pole of the CCF is

$$p_{dom} = \frac{G_4(G_2 + g_m)}{G_4(C_2 + C_3) + G_2(C_4 + C_2) + g_m C_4} . \qquad (12)$$

The transmission zeros of the CCF are so far removed from the origin of the p plane that they do not effect the transient response. The results of substituting parameters into Eq. (12) to obtain the transient response are shown in Section 5.

V. RESULTS

The results of the transient analysis are shown in Figs. 10, 11, and 12. Fig. 10 compares the rise time of the pentode WCF to the pentode CCF (both with the same source and load admittance) as the source resistance is varied. Also shown in Fig. 10 are the experimental results for a triode WCF. The triode case will be discussed in the next section, and all further reference to the WCF in this section is to the pentode case.

The constant parameters for Fig. 10 are R_3, the feedback resistance, and R_L, the load resistance, which are 3900 ohms and 125 ohms respectively. The g_m is equal to 5000 μmhos. The rise time of both the WCF and CCF increases as the source resistance increases. This result is, of course, to be expected because the source resistance together with the input capacitance of the cathode follower functions as an integrator. However, there is an advantage in using the WCF. If the source resistance is greater than about 1000 ohms, the WCF rise time is faster than the CCF by a factor of two.

Figure 11 shows the effect on the transient response of the WCF as the feedback resistor, R_3, is varied. An additional parameter in this case is R_4 equal to either 125 ohms or 1000 ohms. The load resistance is 125 ohms. The rather interesting conclusion to be drawn from Fig. 11 is that, provided a minimal amount of feedback is supplied by R_3, the transient response is relatively insensitive to its value. Because the dc analysis of the WCF shows that a high R_3 leads to low output impedance, it appears that R_3 should be made as large as possible subject to retaining

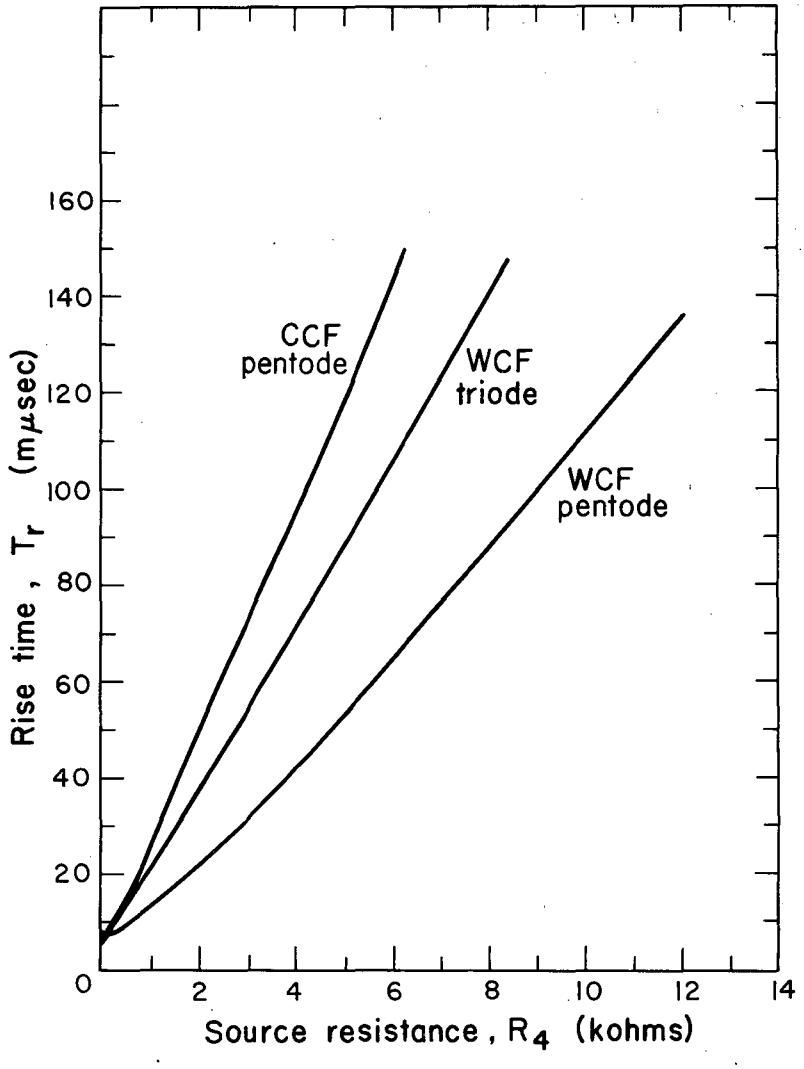

Fig. 10. The effect on the transient response of the WCF and CCF as the source resistance is varied. R_3 equals 3900 ohms and R_L equals 125 ohms.

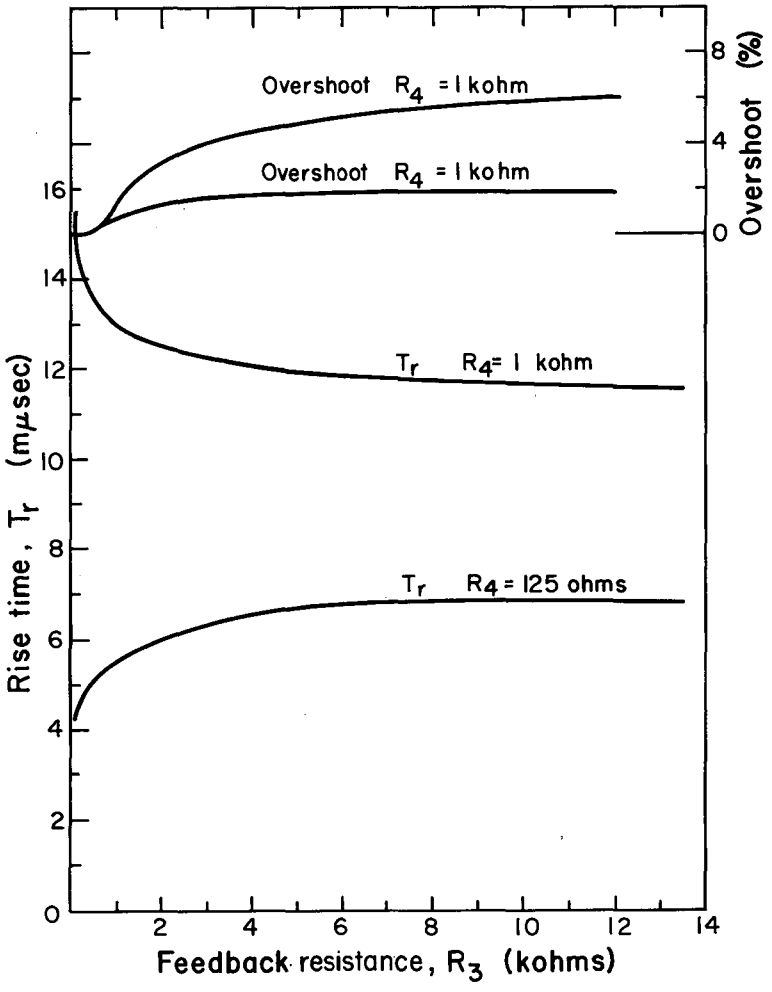

Fig. 11. The effect on the transient response of the WCF as the feedback resistance is varied. R_L equals 125 ohms.

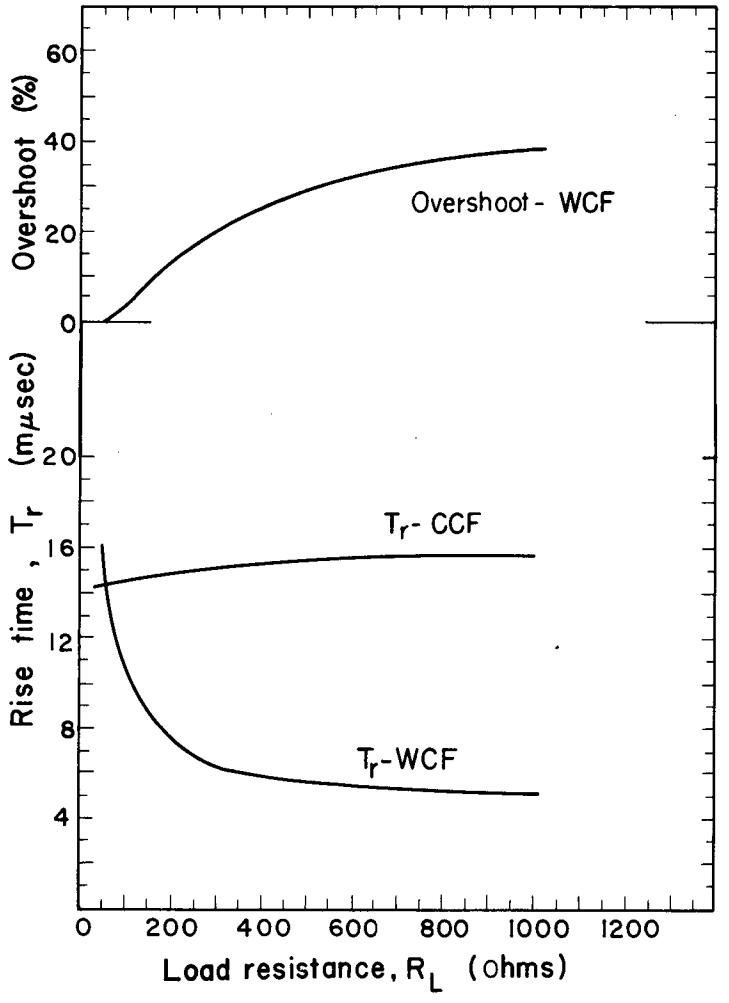

Fig. 12. The effect on the transient response of the WCF and CCF as the load resistance is varied. R_4 equals 500 ohms.

normal plate current and transconductance of the tubes.

Also shown in Fig. 11 is the overshoot as a function of R_3. Overshoot is here defined in percent excursion of the waveform above the final flat top of the step output. If the step output reaches a final dc level of 1 volt and the overshoot is 0.1 volt, the overshoot is 10%. It may be observed that the overshoot is relatively insensitive to the value of R_3 and that its maximum value is about 6%.

Figure 12 shows the effect on the transient response of varying the load resistance of both the WCF and CCF. The source resistor in both cases is 500 ohms. The WCF feedback resistor, R_3, is 3900 ohms.

The CCF curve is nearly flat as the load resistance increases. This may be attributed to the fact that the 200-ohm output impedance is in parallel with the load resistance thus constraining the combination to be no higher than 200 ohms. Inspection of Eq. (12) will substantiate this for high values of load resistance. The situation with the WCF is more complicated.

The WCF exhibits considerable overshoot (up to 40%) and decreased rise time as the load resistance increases. For certain applications the large overshoot may be excessive, indicating that the load resistance should be made smaller. Conversely, if fast rise time is the major consideration, a larger load resistance will help provide for it. Also it should be noted that for a load resistance greater than about 400 ohms, the WCF rise time is three times faster than that of the CCF.

Sufficient information is now available to compare the gain bandwidth of the WCF and the CCF for particular parameters. For the present case let R_3 be equal to 3900 ohms, R_L be equal to 125 ohms, and R_4 be greater than 1000 ohms. Then from the dc analysis the WCF shows a dc gain advantage by a factor of 2.42 over the CCF. As discussed in the transient analysis, the WCF shows an advantage in rise time by a factor of 2 over the CCF. Hence the over-all advantage in gain bandwidth (or gain/rise time) is $2 \times 2.42 \approx 5$.

VI. FURTHER DISCUSSION

The results of Fig. 10 illustrate somewhat of a paradox. While a cathode follower is usually considered a device for transforming a high input impedance to a low output impedance, the high input impedance should be avoided when a fast transient response is desired.

Experimental verification of the curves in Section 5 has been obtained using methods shown in Part I. The maximum error between the experimental and theoretical results is 20%. In the pentode WCF the screens of both tubes were bypassed to their cathodes.

While all of the above work refers only to pentodes, it has been verified experimentally that the conclusions as to the effects of the various resistances hold for triodes. In Fig. 10 is shown the experimental results obtained by bypassing both screens of the 6AK5 WCF to the respective anodes, thereby obtaining a triode WCF. As shown in Fig. 10, the rise time of the triode WCF increased by 65% over the pentode WCF. When the CCF screen was bypassed to its anode, the rise time increased by only a few percent. The difference in the effects may be attributed to the greatly increased Miller capacitance in the triode WCF case. In short, when a fast rise time is the major criterion, triodes are not recommended for the WCF.

Appendix A. WCF Transient Analysis

The nodal equations for the equivalent circuit of the WCF, Fig. 7, are

$$V_1\left[G_1 + G_2 + g_m + p(C_1 + C_2 + C_6)\right] - V_2\left[G_1 - g_m + pC_1\right] - V_3\left[g_m + pC_6\right] = 0.$$

$$-V_1\left[G_1 + g_m + pC_1\right] + V_2\left[G_1 + G_3 + p(C_1 + C_3 + C_5)\right] + V_3\left[g_m - pC_5\right] = 0,$$

and

$$-V_1\left[pC_6\right] - V_2\left[pC_5\right] + V_3\left[G_4 + p(C_4 + C_5 + C_6)\right] = I_{in}. \qquad \text{(A-1)}$$

By the use of Cramer's rule with Eqs. (A-1), the transfer function of the WCF is (with $V_{in} = I_{in}/G_4$)

$$\frac{V_1}{V_{in}} = \frac{G_4\left\{ p^2\left[C_6(C_1 + C_3 + C_5) + C_1C_5\right] + p\left[C_6(G_1 + G_3) + C_3g_m\right] + g_m^2 + G_3g_m\right\}}{\Delta} \qquad \text{(A-2)}$$

where Δ is the system determinant given by

$$p^3\left\{C_5\left[\begin{array}{l} C_1C_4 + C_2C_4 + C_6C_4 \\ + C_1C_3 + C_2C_3 + C_3C_6 \\ + C_1C_2 + C_2C_6 \end{array}\right] + C_4\left[\begin{array}{l} C_1C_3 + C_2C_3 + C_3C_6 \\ + C_1C_2 + C_1C_6 \end{array}\right] + C_6\left[C_1C_3 + C_2C_3 + C_1C_2\right]\right\}$$

$$+p^2\left\{C_5\left[\begin{array}{l} C_4G_1 + C_4G_2 + C_4g_m + C_3G_1 + C_3G_2 + C_3g_m \\ + C_1G_3 + C_2G_3 + C_6G_3 + C_2G_1 + C_1g_m + C_1G_2 \\ + C_6G_2 + C_6g_m + C_1G_4 + C_2G_4 + C_6G_4 + C_2g_m \end{array}\right]\right.$$

$$+ C_4\left[\begin{array}{l} C_3G_1 + C_3G_2 + C_3g_m + C_1G_3 + C_2G_3 + C_6G_3 \\ + C_2G_1 + C_6G_1 + C_1g_m + C_1G_2 \end{array}\right]$$

$$+ C_6\left[\begin{array}{l} C_3G_1 + C_3G_2 + C_1G_3 + C_2G_3 + C_2G_1 + C_1g_m \\ + C_1G_2 + C_3G_4 + C_1G_4 \end{array}\right]$$

$$\left. + G_4\left[C_1C_2 + C_3C_2 + C_1C_3\right]\right\}$$

$$+p\left\{C_5\left[\begin{array}{l} G_3G_1 + G_3G_2 + G_3g_m + G_1G_2 + g_m^2 + G_1g_m \\ + G_1G_4 + G_2G_4 + G_4g_m + G_2g_m \end{array}\right]\right.$$

$$+ C_4\left[G_3G_1 + G_3G_2 + G_3g_m + G_1G_2 + g_m^2 + G_1g_m\right]$$
$$+ C_6\left[G_3G_1 + G_3G_2 + G_1G_2 + G_1g_m + G_3G_4 + G_1G_4\right]$$
$$+ G_4\left[\begin{matrix}C_3G_1 + C_3G_2 + C_3g_m + C_1G_3 + C_2G_3 + \\ C_2G_1 + C_1g_m + C_1G_2\end{matrix}\right]\Bigg\}$$
$$+ G_4\left[G_3G_1 + G_3G_2 + G_3g_m + G_1G_2 + g_m^2 + G_1g_m\right].$$

The roots of the denominator of Eq. (A-2) are the poles of the transfer function. The roots of the numerator are the transmission zeros.

Appendix B. CCF Transient Analysis

The nodal equations for the equivalent circuit of the CCF, Fig. 9, are

$$V_1\left[p(C_2 + C_4) + G_4\right] - V_2\left[pC_2\right] = I_{in}$$

and

$$-V_1\left[pC_2 + g_m\right] + V_2\left[p(C_2 + C_3) + G_2 + g_m\right] = 0. \qquad \text{(B-1)}$$

If we apply Cramer's rule to Eqs. (B-1), the transfer function of the CCF is (with $V_{in} = I_{in}/G_4$)

$$\frac{V_2}{V_{in}} = \frac{G_4(pC_2 + g_m)}{\Delta}\ , \qquad \text{(B-2)}$$

where Δ, the system determinant, is given by

$$p^2\left[C_3(C_2 + C_4) + C_2C_4\right] + p\left[G_4(C_2 + C_3) + G_2(C_2 + C_4) + g_mC_4\right]$$
$$+ \left[G_4(G_2 + g_m)\right].$$

REFERENCES

1. Radiotron Designer's Handbook, F. Langford-Smith, Ed., (Amalgamated Wireless Valve Company Pty. Ltd., Sydney, Australia, 1952) p. 400. Thirty-two references are listed.
2. E. L C. White, Thermionic Valve Amplifier Circuit Arrangements, U. S. Patent No. 2,358,428, September 19, 1944.
3. Calvin M. Hammack in The Electron Art, Frank Rockett, Ed., Electronics 19, 206 (Nov. 1946).
4. Moody, Battell, Howell, and Taplin, Rev. Sci. Instr. 22, 557 (1951).
5. E. Fairstein, Rev. Sci. Instr. 27, 475 (1956).
6. A. S. Penfold, Rev. Sci, Instr. 29, 765 (1958).
7. E. L. Garwin, Rev. Sci. Instr. 30, 373 (1959).
8. The problem is not intractable. See B. Y. Mills, Proc. I. R. E. 37, 631 (1949).
9. Melvin Brown, Rev. Sci. Instr. 30, 169 (1959).
10. D. O. Pederson and G. W. Wilson, Delay Time In Dominant-Pole Circuits, Electronics Research Laboratory, Department of Electrical Engineering, University of California, Berkeley, Calif., Report No. 80, Series No. 60, February 5, 1959.
11. Handbook of Automation, Computation, and Control, Vol. 1, Eugene M. Grabbe, Simon Ramo, and Dean E. Wooldridge, Eds. (John Wiley and Sons, Inc., New York, 1958), p. 22-04.
12. J. G. Linvill, Proc. I. R. E. 43, 826 (1955).
13. See reference 11, p. 22-39
14. See for example, Samuel Seely, Electronic Engineering, (McGraw-Hill Book Company, Inc., New York, 1956), p. 137.

ACKNOWLEDGMENT

Discussions during the course of this work with Prof. Donald O. Pederson of the Electrical Engineering Department of the University of California have been most valuable. Thanks are also due Michiyuki Nakamura of the Lawrence Radiation Laboratory for introducing the author to the possibilities of the DPL in trigger circuits.

This work was done under the auspices of the U. S. Atomic Energy Commission.